PHYSICAL REVIEW D **96,** 015040 (2017)

One-loop renormalization of the NMSSM in SloopS. II. The Higgs sector

G. Bélanger,[1,*] V. Bizouard,[1,†] F. Boudjema,[1,‡] and G. Chalons[2,§]

[1]*LAPTh, Université Savoie Mont Blanc, CNRS, B.P.110, F-74941 Annecy-le-Vieux Cedex, France*
[2]*LPT (UMR8627), CNRS, Université Paris-Sud, Université Paris-Saclay, 91045 Orsay, France*

(Received 12 May 2017; published 31 July 2017)

We present a full one-loop renormalization of the Higgs sector of the next-to-minimal-supersymmetric-Standard-Model (NMSSM) and its implementation within SloopS, a code for the automated computations of one-loop processes in theories beyond the Standard Model. The present work is the sequel to the study we performed on the renormalization of the sectors of the NMSSM comprising neutralinos, charginos, and sfermions, thereby completing the full one-loop renormalization of the NMSSM. We have investigated several renormalization schemes based on alternative choices (on-shell or $\overline{\text{DR}}$) of the physical parameters. Special attention is paid to the issue of the mixing between physical fields. To weigh the impact of the different renormalization schemes, the partial widths for the decays of the Higgs bosons into supersymmetric particles are computed at one loop. In many decays large differences between the schemes are found. We discuss the origin of these differences. In particular, we study two contrasting scenarios. The first model is MSSM-like with a small value for the mixing between the doublet and singlet Higgs superfields while the second model has a moderate value for this mixing. We critically discuss the issue of the reconstruction of the underlying parameters and their counterterms in the case of a theory with a large number of parameters, such as the NMSSM, from a set of physical parameters. In the present study this set corresponds to the minimum set of masses for the implementation of the on-shell schemes.

DOI: 10.1103/PhysRevD.96.015040

I. INTRODUCTION

The discovery of a Standard Model-like Higgs boson at the LHC [1,2] has raised some concerns with one of the favorite extensions of the Standard Model (SM), the minimal supersymmetric Standard Model (MSSM). A Higgs mass of 125 GeV, near the maximum value achievable in this model, requires some fine-tuning [3]. In a minimal singlet extension of the model with a $\mathbb{Z}_3$ symmetry, the next-to-MSSM (NMSSM), additional Higgs quartic couplings allow one to raise the tree-level mass of the SM-like Higgs [4,5], hence reducing both the amount of radiative corrections required from the top/stop sector and the amount of fine-tuning [6–8]. In addition, this model provides a natural explanation for the scale of the Higgsino parameter μ, by relating it to the vacuum expectation value (VEV), of the scalar singlet, thus solving the little hierarchy problem of the MSSM.

The computation of higher-order corrections to Higgs production at the LHC as well as its decay rates has been a field of intense activity for the past two decades, in particular for the SM Higgs; for an update see [9–12]. The bulk of the corrections have to do with QCD corrections. For the MSSM, the best example for the importance of the higher order corrections in the Higgs sector is the correction to the Higgs mass [13,14]. Without these corrections driven by the top mass, the MSSM would not have survived for so long [15–18]. Many of these computations have been extended and/or adapted to the case of the NMSSM, in particular for the Higgs masses [19–25] with improvements including several two-loop effects [26–30]. Adaptations of the computations of higher order corrections for Higgs production at the LHC from the SM and the MSSM to the NMSSM have been performed [31]. One-loop corrections to Higgs decays in the NMSSM have also been considered with varying degrees of generalization and approximation depending on the final state. Full QCD/supersymmetric-QCD (SUSY-QCD) corrections to decays to SM fermions [32] have been performed, as well as electroweak and QCD corrections to channels such as the decays of *CP*-odd Higgses into stops [33] and Higgs self-couplings [34], while many other channels such as decays to neutralinos and charginos have been adapted from the MSSM [35]. Some electroweak corrections are still not fully systematically included for all decays. Many of these one-loop (or in the case of masses beyond one-loop) corrections have been incorporated into several public codes for the NMSSM: NMSSMTools [36,37], SPheno [38,39], NMSDECAY [40], SoftSUSY [41], NMSSMCALC [35], and FlexibleSUSY [42]. Most of these computations are based on a $\overline{\text{DR}}$ scheme or on a mixed $\overline{\text{DR}}$/on-shell (OS) scheme as in NMSSMCALC [35]. In principle an automated implementation of two-body decays in $\overline{\text{DR}}$ of the NMSSM could be attempted for the NMSSM along the lines described in [43]. A full OS scheme at one loop for the NMSSM has not been studied.

*belanger@lapth.cnrs.fr
†vincent.bizouard2@gmail.com
‡boudjema@lapth.cnrs.fr
§guillaume.chalons@th.u-psud.fr

One of the aims of this paper is to precisely implement different renormalization schemes including a few variants of a full OS scheme in order to perform complete one-loop corrections for *any* process in the NMSSM. We have shown in a previous paper [44] how such a program is applied to the renormalization of the neutralino/chargino and sfermion sectors of the NMSSM, and we extend it here to cover the Higgs sector. Because of the role played by the effective μ parameter in the NMSSM, or in other words, the doublet-singlet λ mixing, there is a strong interconnection between the chargino/neutralino sector and the Higgs sector, which warrants a common and overall coherent approach to the complete one-loop renormalization of the NMSSM. This work is a natural extension of the work done for the MSSM in [45,46] where, after performing the complete renormalization of the MSSM, one-loop corrections to masses, two-body decays, and production cross sections at colliders were computed together with one-loop corrections for various dark matter annihilation processes [47–49]. The fact that one is able to perform one-loop corrections to a host of processes is made possible by the implementation of the theoretical setup for the one-loop renormalization in SloopS, a code for the automated generation and evaluation of any cross section. The one-loop theoretical setup will be detailed here. As a prerequisite for SloopS, one first needs to read a model file. The model file, the NMSSM in this case, is obtained automatically with an improved version of LanHEP [50–52] that allows for the generation of the counterterms and the corresponding Feynman rules. The code then relies on FeynArts [53], FormCalC [54], and LoopTools for the automatic computation of one-loop processes [55], including both electroweak and QCD corrections. Preliminary applications of SloopS to the NMSSM dealt with computing one-loop induced decays into photons: (i) neutralino annihilations into photons, the gamma-ray lines for dark matter indirect detection [56,57], and (ii) Higgs decays to photons at the LHC [58,59]. These processes do not call for counterterms or renormalization at one loop, yet an important part of the machinery of SloopS is called for.

The NMSSM is a typical beyond the SM theory with many parameters, fields, and mixings where the different sectors are intertwined. The vast majority of its parameters, as they appear at the level of the Lagrangian, are not directly measurable in experiments in the sense that there is not a straightforward linear mapping between these parameters and an observable such as a mass. The reconstruction of these parameters is a real challenge even when attempted at tree level. Renormalization being tightly linked to the choice of input parameters to be extracted from experimental measurements, having currently no sign of supersymmetry, leaves this choice with no clear guidance. However, the current extensive program of precision measurements of the Higgs couplings at the LHC requires nonetheless precise theoretical predictions making the renormalization of the Higgs sector of the NMSSM highly desirable. As for the neutralino/chargino sector that we studied in [44], different schemes are possible. We use mostly on-shell schemes where input parameters are taken from the masses of the neutralino/chargino and from the Higgs sectors. In such schemes, based on two-point functions only, the task of renormalizing the model boils down to choosing a minimal/sufficient set of physical masses as input parameters. In this work, we have adopted several sets of input parameters and discussed how efficiently each set can constrain the needed counterterms to keep the radiative corrections under control. Moreover, the renormalization procedure induces additional mixing, not only among the Higgs physical states but also new gauge-Higgs and Goldstone-Higgs transitions in the pseudoscalar and charged sector appear. Such mixing must vanish for on-shell physical states by imposing appropriate conditions on the wave function renormalization constants, which have to satisfy Ward-Slavnov-Taylor (WST) identities. In doing so we have rederived the WST identities governing the $A_i^0 Z^0/H^{\pm}W^{\pm}$ mixing in the NMSSM.

The dependence on the renormalization scheme is then illustrated in numerical computations of observables. Full one-loop electroweak corrections to decays of Higgs particles are computed. The scheme dependence for Higgs to Higgs decays and for decays involving charginos/neutralinos is carefully examined. Note that while the Higgs mass computation is not as accurate as in other codes (only one-loop corrections are included), we nevertheless stress that our approach allows for a consistent treatment of on-shell renormalization and one-loop corrections to masses, decays, and scattering processes. This is of importance given the very precise experimental measurements achieved both for the Higgs and for dark matter waobservables.

The paper is organized as follows. Section II contains a description of the Higgs sector of the NMSSM and enumerates the number of fields and parameters that will need renormalization. The needed counterterms to obtain ultraviolet finite results are introduced in Sec. III, and in the following section the issue of mixing in the Higgs sector through the self-energies is discussed. Section V presents the different renormalization schemes that enable a reconstruction of the counterterms of the underlying parameters the NMSSM with a special attention to those of the Higgs sector. Section VI presents how the numerical results are checked and how the scheme dependence can be quantified in order to gain insights on the theoretical uncertainties. In Sec. VII we present two scenarios for which, in Sec. VIII, we compute numerically several Higgs partial widths and discuss their scheme dependence. Finally our conclusions are made in Sec. IX.

II. THE HIGGS SECTOR OF THE NMSSM

A. Fields and potential

The NMSSM contains three Higgs superfields: two $SU(2)_L$ doublets $\hat{H}_u$ and $\hat{H}_d$, as in the MSSM, and one additional gauge singlet $\hat{S}$

$$\hat{H}_u = \begin{pmatrix} \hat{H}_u^+ \\ \hat{H}_u^0 \end{pmatrix}, \qquad \hat{H}_d = \begin{pmatrix} \hat{H}_d^0 \\ \hat{H}_d^- \end{pmatrix}, \qquad \hat{S}. \quad (2.1)$$

In the $\mathbb{Z}_3$ implementation that we will assume, the Higgs superpotential is made up of two operators, associated with the dimensionless couplings λ and κ,

$$W_{\rm Higgs} = -\lambda \hat{S}\hat{H}_d \cdot \hat{H}_u + \frac{1}{3}\kappa \hat{S}^3, \quad (2.2)$$

where $\hat{H}_d \cdot \hat{H}_u = \epsilon_{ab}\hat{H}_d^a \hat{H}_u^b$ and ϵ_{ab} is the two-dimensional Levi-Cività symbol with $\epsilon_{12} = 1$. The two parameters λ and κ of the superpotential will, by construction, affect the phenomenology of both the Higgs and chargino/neutralino sectors. The five neutralinos of the NMSSM will be an admixture of the (i) $SU(2)$, $\tilde{w}$, and $U(1)$, $\tilde{b}$, neutral gauginos; (ii) the two neutral Higgsinos, $\tilde{h}_{u,d}$, the fermionic components of two superfields $\hat{H}_{u,d}$; and (iii) the singlino, $\tilde{s}$, the fermionic component of $\hat{S}$. λ in particular is crucial; it not only is necessary in order to induce the μ term but it also gives rise to mixing in the neutralino sector as well as in the Higgs sector between the Higgs doublets and the new singlet. In passing we recall that μ sets the mass scale for the Higgsinos; see [44] for more detail. For the purpose of parameter counting and of the renormalization of the Higgs sector at one loop there is no need to go over the Yukawa superpotential which we have given in the previous paper [44]. However, we do need to clearly specify again the soft SUSY breaking Lagrangian, in particular the part relating to the Higgs sector,

$$-\mathcal{L}_{\rm soft,scalar} = m_{H_u}^2 |H_u|^2 + m_{H_d}^2 |H_d|^2 + m_S^2 |S|^2 + \left(\lambda A_\lambda H_u \cdot H_d S + \frac{1}{3}\kappa A_\kappa S^3 + \text{H.c.}\right). \quad (2.3)$$

The first two terms in the first line represent the soft mass terms for the Higgs doublets and the third, not present in the MSSM, of the singlet. The second line, not present in the MSSM also, represents the NMSSM trilinear Higgs couplings A_κ, A_λ. A_λ affects the mixing between the Higgs doublets and the singlet, beside the mixing introduced by λ. This parameter plays an important role in the phenomenology of the Higgs sector in the NMSSM; note that it gives rise to a Higgs trilinear coupling $H_u H_d S$. No source of CP violation is assumed.

We are now in a position to write the Higgs potential whose parameters will need to be renormalized. With g, g' being, respectively, the $SU(2)$ weak and $U(1)$ hypercharge gauge couplings and specifying the components of the doublets,

$$H_d = \begin{pmatrix} H_d^0 \\ H_d^- \end{pmatrix} \qquad H_u = \begin{pmatrix} H_u^+ \\ H_u^0 \end{pmatrix},$$

the potential reads

$$\begin{aligned} V_{\rm Higgs} = {} & |\lambda(H_u^+ H_d^- - H_u^0 H_d^0) + \kappa S^2|^2 + (m_{H_u}^2 + |\lambda S|^2)(|H_u^0|^2 + |H_u^+|^2) + (m_{H_d}^2 + |\lambda S|^2)(|H_d^0|^2 + |H_d^+|^2) \\ & + \frac{g^2 + g'^2}{8}(|H_u^0|^2 + |H_u^+|^2 - |H_d^0|^2 - |H_d^-|^2)^2 + \frac{g^2}{2}|H_u^+ H_d^{0*} + H_u^0 H_d^{-*}|^2 + m_S^2 |S|^2 \\ & + \left(\lambda A_\lambda (H_u^+ H_d^- - H_u^0 H_d^0) S + \frac{1}{3}\kappa A_\kappa S^3 + \text{H.c.}\right). \end{aligned} \quad (2.4)$$

Electroweak symmetry breaking occurs for appropriate values of the soft terms. The Higgs fields are expanded around their vacuum expectation values,

$$H_d = \begin{pmatrix} v_d + \frac{h_d^0 + i a_d^0}{\sqrt{2}} \\ h_d^- \end{pmatrix}, \quad (2.5)$$

$$H_u = \begin{pmatrix} h_u^+ \\ v_u + \frac{h_u^0 + i a_u^0}{\sqrt{2}} \end{pmatrix}, \quad (2.6)$$

$$S = s + \frac{h_s^0 + i a_s^0}{\sqrt{2}}. \quad (2.7)$$

The vacuum expectation values, v_u, v_d, s are chosen to be real and positive. As in the MSSM we define

$$v^2 = v_u^2 + v_d^2, \quad \tan\beta \equiv t_\beta = v_u/v_d \quad (v_{u,d} = v s_\beta, v c_\beta), \quad (2.8)$$

such that the W mass is

$$M_W^2 = g^2 v^2/2. \quad (2.9)$$

The nonvanishing value of the VEV of S also gives a solution to the so-called μ problem of the MSSM by generating this parameter dynamically,

$$\mu_{\rm eff} = \lambda s. \quad (2.10)$$

We define $\mu_{\rm eff} = \mu$ in the following and will take it as an independent parameter, where comparison with the MSSM

will then be easier. In addition to μ, we take λ and κ as independent parameters while s is kept as a shorthand notation for μ/λ in the same way as we use c_W as a shorthand notation for M_W/M_Z. It is useful to introduce the combinations

$$\Lambda_v = \lambda v \quad \text{and}$$
$$m_\kappa = \kappa s = (\kappa/\lambda)\mu. \tag{2.11}$$

With these parameters, the MSSM limit is obtained by taking $\kappa, \lambda(\Lambda_v) \to 0$, while keeping μ fixed such that the mass of the Higgsinos is $|\mu|$. The reason we take m_κ is that the mass of the singlinolike neutralino is a substitute for m_κ. Indeed, in the MSSM limit, the singlino mass is (see [44])

$$m_{\tilde{s}} = 2m_\kappa. \tag{2.12}$$

At the minimum of the potential, the part of the potential linear in any of the CP-even Higgs fields has to vanish, $\partial V_{H_{\rm Higgs}}/\partial h_i^0 = 0$. It can be written in terms of the tree-level tadpoles,

$$\begin{aligned}
\frac{\mathcal{T}_{h_d^0}}{2v_d} &= -\mu t_\beta(A_\lambda + m_\kappa) + \Lambda_v^2 s_\beta^2 + (m_{H_d}^2 + \mu^2) + \frac{M_Z^2}{2}c_{2\beta},\\
\frac{\mathcal{T}_{h_u^0}}{2v_u} &= -\frac{\mu}{t_\beta}(A_\lambda + m_\kappa) + \Lambda_v^2 c_\beta^2 + (m_{H_u}^2 + \mu^2) - \frac{M_Z^2}{2}c_{2\beta},\\
\frac{\mathcal{T}_{h_s^0}}{2s} &= m_\kappa(A_\kappa + 2m_\kappa) + \Lambda_v^2\left(1 - s_{2\beta}\frac{A_\lambda + 2m_\kappa}{2\mu}\right) + m_S^2.
\end{aligned} \tag{2.13}$$

The conditions on the vanishing of the three tadpoles allow us to express the soft mass terms $m_{H_d}^2, m_{H_u}^2, m_S^2$ in terms of the tadpoles.

The quadratic part of the Higgs potential, bilinear in the fields, gives rise to the mass terms for the Higgs sector,

$$\begin{aligned}
V_{\rm mass} = &\frac{1}{2}(h^0)^T \cdot M_S^2 \cdot h^0 + \frac{1}{2}(a^0)^T \cdot M_P^2 \cdot a^0\\
&+ h^- \cdot M_\pm^2 \cdot h^+,
\end{aligned} \tag{2.14}$$

with

$$(h^0)^T = (\, h_d^0 \quad h_u^0 \quad h_s^0\,), \tag{2.15}$$

$$(a^0)^T = (\, a_d^0 \quad a_u^0 \quad a_s^0\,), \tag{2.16}$$

$$(h^\pm)^T = (\, h_d^\pm \quad h_u^\pm\,), \tag{2.17}$$

and where M_S^2, M_P^2, and $M_\pm^2$ are, respectively, the mass matrices for the CP-even, the CP-odd, and the charged Higgs bosons.

The charged Higgs

The mass matrix for the charged Higgs, $M_\pm^2$, reads

$$\begin{aligned}
M_\pm^2 = &\frac{1}{2}\begin{pmatrix} \frac{\mathcal{T}_{h_d^0}}{v_d} & 0 \\ 0 & \frac{\mathcal{T}_{h_u^0}}{v_u} \end{pmatrix} + \left(\mu(A_\lambda + m_\kappa) + \frac{s_{2\beta}}{2}(M_W^2 - \Lambda_v^2)\right)\\
&\times \begin{pmatrix} t_\beta & 1 \\ 1 & 1/t_\beta \end{pmatrix}.
\end{aligned} \tag{2.18}$$

With the tadpoles set to zero [using the tree-level condition in Eq. (2.13)], we have $\mathrm{Det}M_\pm^2 = 0$ which signals the presence of a massless charged Goldstone boson. The mass of the physical charged Higgs boson is given by the trace of $M_\pm^2$,

$$M_{H^\pm}^2 = \underbrace{\frac{2\mu}{s_{2\beta}}(A_\lambda + m_\kappa)}_{M_A^2 = M_{A,\rm MSSM}^2} + (M_W^2 - \Lambda_v^2). \tag{2.19}$$

The MSSM limit is obtained by letting Λ_v to 0 in the above, while all other parameters are fixed. What is denoted M_A is the equivalent of the pseudoscalar mass in the MSSM limit. Note that if $m_\kappa(\kappa), \Lambda_v(\lambda), \mu$, and t_β have been extracted from the chargino/neutralino sector, the measurement of the charged Higgs mass reconstructs A_λ. As explained in [44], for this to work efficiently t_β should not be too large and in all cases should be well measured. The charged Higgs mass could also serve for the measurement of t_β if A_λ is determined from the other Higgs masses.

The diagonalizing matrix, $U(\beta)$, to obtain the Goldstone and physical charged Higgs is defined as

$$\mathcal{H}^\pm \equiv \begin{pmatrix} G^\pm \\ H^\pm \end{pmatrix} = U_\beta h^\pm = U_\beta \begin{pmatrix} h_d^\pm \\ h_u^\pm \end{pmatrix}, \tag{2.20}$$

with

$$U_\beta = \begin{pmatrix} c_\beta & -s_\beta \\ s_\beta & c_\beta \end{pmatrix}. \tag{2.21}$$

The pseudoscalars

The pseudoscalar mass matrix, M_P^2, decomposes into the following elements:

$$\begin{aligned}
M_{P_{11}}^2 &= \frac{\mathcal{T}_{h_d^0}}{2v_d} + \mu t_\beta(A_\lambda + m_\kappa),\\
M_{P_{22}}^2 &= \frac{\mathcal{T}_{h_u^0}}{2v_u} + \frac{\mu}{t_\beta}(A_\lambda + m_\kappa),\\
M_{P_{33}}^2 &= \frac{\mathcal{T}_{h_s^0}}{2s} + \Lambda_v^2\frac{A_\lambda + 4m_\kappa}{2\mu}s_{2\beta} - 3m_\kappa A_\kappa,\\
M_{P_{12}}^2 &= M_{P_{21}}^2 = \mu(A_\lambda + m_\kappa),\\
M_{P_{13}}^2 &= M_{P_{31}}^2 = \Lambda_v(A_\lambda - 2m_\kappa)s_\beta,\\
M_{P_{23}}^2 &= M_{P_{32}}^2 = \Lambda_v(A_\lambda - 2m_\kappa)c_\beta.
\end{aligned} \tag{2.22}$$

As expected, upon setting the tadpole to zero, $\mathrm{Det}M_P^2 = 0$. This reveals the neutral Goldstone boson. With the 2×2 submatrix, m_{12}^2

$$m_{12}^2 = s_\beta c_\beta M_{A,\mathrm{MSSM}}^2 \begin{pmatrix} t_\beta & 1 \\ 1 & 1/t_\beta \end{pmatrix},$$
$$\mathrm{Tr}(m_{12}^2) = M_{A,\mathrm{MSSM}}^2, \tag{2.23}$$

in the MSSM limit ($\Lambda_v \to 0$) we have

$$M_P^2 \to \begin{pmatrix} m_{12}^2 & 0 \\ 0 & -3m_\kappa A_\kappa \end{pmatrix}. \tag{2.24}$$

The Goldstone boson can be isolated through the 3×3 extension of the matrix U_β encountered for the charged Higgs sector

$$U^{(3)}(\beta) = \begin{pmatrix} c_\beta & -s_\beta & 0 \\ s_\beta & c_\beta & 0 \\ 0 & 0 & 1 \end{pmatrix}. \tag{2.25}$$

In this new basis where the Goldstone boson is separated, the pseudoscalar mass matrix simplifies to

$$U^{(3)}(\beta) M_P^2 U^{(3)}(\beta)^\dagger = \begin{pmatrix} 0 & 0 & 0 \\ 0 & & \\ 0 & & \hat{M}_P^2 \end{pmatrix}, \tag{2.26}$$

where the (2×2) mixing matrix between the two pseudoscalar bosons is given by

$$\hat{M}_P^2 = \begin{pmatrix} M_A^2 & \Lambda_v(A_\lambda - 2m_\kappa) \\ \Lambda_v(A_\lambda - 2m_\kappa) & \Lambda_v^2 \frac{A_\lambda + 4m_\kappa}{2\mu} s_{2\beta} - 3m_\kappa A_\kappa \end{pmatrix}. \tag{2.27}$$

The MSSM limit is clearly exhibited. Diagonalization of this matrix is then performed through a 2×2 matrix $\hat{P}_a$ which we can parametrize as

$$\hat{P}_a = \begin{pmatrix} c_p & -s_p \\ s_p & c_p \end{pmatrix}. \tag{2.28}$$

Putting everything together the pseudoscalar mass matrix is diagonalized through the matrix P_a,

$$P_a = \underbrace{\begin{pmatrix} 1 & 0 & 0 \\ 0 & & \\ 0 & & \hat{P}_a \end{pmatrix}}_{\hat{P}_a^{(3)}} U^{(3)}(\beta) = \begin{pmatrix} c_\beta & -s_\beta & 0 \\ c_p s_\beta & c_p c_\beta & -s_p \\ s_p s_\beta & s_p c_\beta & c_p \end{pmatrix}, \tag{2.29}$$

such that

$$\mathcal{P}^0 \equiv \begin{pmatrix} G^0 \\ A_1^0 \\ A_2^0 \end{pmatrix} = P_a a^0 = P_a \begin{pmatrix} a_d^0 \\ a_u^0 \\ a_s^0 \end{pmatrix}. \tag{2.30}$$

It is important to remember that

$$(P_a)_{13} = (P_a^{-1})_{31} = 0 \quad \text{and that}$$
$$(P_a)_{1i} = (U^{(3)}(\beta))_{1i} \quad \text{for } i = 1, 2. \tag{2.31}$$

We will also set $(\mathcal{P}^0)_1 \equiv A_0^0 \equiv G^0$ for the identification of the neutral Goldstone Boson.

The CP-even scalars

The elements of the scalar mass matrix, M_S^2, read

$$\begin{aligned} M_{S_{11}}^2 &= \frac{\mathcal{T}_{h_d^0}}{2v_d} + M_Z^2 c_\beta^2 + M_A^2 s_\beta^2, \\ M_{S_{22}}^2 &= \frac{\mathcal{T}_{h_u^0}}{2v_u} + M_Z^2 s_\beta^2 + M_A^2 c_\beta^2, \\ M_{S_{33}}^2 &= \frac{\mathcal{T}_{h_s^0}}{2s} + \Lambda_v^2 A_\lambda \frac{c_\beta s_\beta}{\mu} + m_\kappa(A_\kappa + 4m_\kappa), \\ M_{S_{12}}^2 &= M_{S_{21}}^2 = (2\Lambda_v^2 - M_Z^2 - M_A^2) s_\beta c_\beta, \\ M_{S_{13}}^2 &= M_{S_{31}}^2 = \Lambda_v(2\mu c_\beta - (A_\lambda + 2m_\kappa) s_\beta), \\ M_{S_{23}}^2 &= M_{S_{32}}^2 = \Lambda_v(2\mu s_\beta - (A_\lambda + 2m_\kappa) c_\beta). \end{aligned} \tag{2.32}$$

To get the physical eigenstates, we introduce the orthogonal matrix S_h, such that

$$\begin{pmatrix} h_1^0 \\ h_2^0 \\ h_3^0 \end{pmatrix} = S_h \begin{pmatrix} h_d^0 \\ h_u^0 \\ h_s^0 \end{pmatrix}. \tag{2.33}$$

We can make the MSSM limit more apparent by writing the diagonalizing matrix of the CP-even Higgs mass matrix, $S_h = \hat{S}_h U^{(3)}(\beta)$. After rotation by $U^{(3)}(\beta)$ an upper limit for the nonsinglet and CP-even lightest neutral Higgs mass is contained in an element of the mass matrix. The upper bound on this mass is

$$M_{h_1^0}^2 < M_Z^2 \left(c_{2\beta}^2 + \frac{\Lambda_v^2}{M_Z^2} s_{2\beta}^2 \right) \equiv M_Z^2 \left(1 + \left(\frac{\Lambda_v^2}{M_Z^2} - 1 \right) s_{2\beta}^2 \right).$$

To have a tree-level mass that is higher than M_Z, Λ_v needs to be larger than M_Z ($\lambda > \sqrt{g^2 + g'^2}/2$). Moreover, the largest tree-level mass corresponds to moderate values of t_β. We need to keep this in mind when we discuss our benchmark points.

It is also useful to write

$$M^2_{h^0_i} = \sum_{j,k=1}^{3} S_{h_{ij}} S_{h_{ik}} M^2_{S_{jk}}, \qquad M^2_{A^0_i} = \sum_{j,k=1}^{3} P_{a_{(i+1)j}} P_{a_{(i+1)k}} M^2_{P_{jk}}. \tag{2.34}$$

The properties of the physical states depend critically on the mixing matrices S_h for the parity-even Higgses and on P_a for the parity-odd Higgses. These mixing matrices, which stem from the nondiagonal nature of the mass matrices/bilinear terms, introduce a highly nonlinear dependence of the couplings involving the Higgses on the underlying parameters of the theory, whereas before mixing, in so to speak the current basis, the functional dependence of the Higgs couplings on the underlying parameters is quite simple, linear or quadratic. This can be seen from the Higgs potential in Eq. (2.7). For example, before these rotation matrices are introduced, the coupling between three different CP-even neutral Higgses ($h^0_d h^0_u h^0_s$) is proportional to $\lambda A_\lambda + 2\kappa\mu = \Lambda_v(A_\lambda + 2m_\kappa)/v$ and hence directly proportional to λ. After moving to the physical basis, the $h^0_1 h^0_2 h^0_3$ coupling is much more complicated since it involves the product of three S_h. Therefore the dependence of this coupling on the underlying parameters is more difficult to track. Since the triple Higgs couplings will enter some of the decays we will study, we write them below for the CP-even Higgs sector,

$$\begin{aligned}
\sqrt{2} v g_{h^0_i h^0_j h^0_k} = {} & \frac{M_Z^2}{2}(c_\beta(\Pi^S)^{1,1,1}_{i,j,k} + s_\beta(\Pi^S)^{2,2,2}_{i,j,k}) + \left(\Lambda_v^2 - \frac{M_Z^2}{2}\right)(c_\beta(\Pi^S)^{1,2,2}_{i,j,k} + s_\beta(\Pi^S)^{2,1,1}_{i,j,k}) \\
& + \Lambda_v^2\left(\left(c_\beta - \frac{m_\kappa}{\mu}s_\beta\right)(\Pi^S)^{1,3,3}_{i,j,k} + \left(s_\beta - \frac{m_\kappa}{\mu}c_\beta\right)(\Pi^S)^{2,3,3}_{i,j,k}\right) \\
& + \Lambda_v\left(\mu((\Pi^S)^{3,1,1}_{i,j,k} + (\Pi^S)^{3,2,2}_{i,j,k}) - (A_\lambda + 2m_\kappa)(\Pi^S)^{3,1,2}_{i,j,k} + \frac{m_\kappa}{\mu}\frac{A_\kappa + 6m_\kappa}{3}(\Pi^S)^{3,3,3}_{i,j,k}\right),
\end{aligned} \tag{2.35}$$

where the Π^S represent the product of three S_h,

$$\begin{aligned}
(\Pi^S)^{a,b,c}_{i,j,k} = {} & S_{h_{ia}}(S_{h_{jb}}S_{h_{kc}} + S_{h_{jc}}S_{h_{kb}}) \\
& + S_{h_{ib}}(S_{h_{ja}}S_{h_{kc}} + S_{h_{jc}}S_{h_{ka}}) \\
& + S_{h_{ic}}(S_{h_{ja}}S_{h_{kb}} + S_{h_{jb}}S_{h_{ka}}).
\end{aligned} \tag{2.36}$$

In the case where mixing is neglected in S_h we have

$$\begin{aligned}
(\Pi^S)^{a,b,c}_{i,j,k} = {} & \delta_{ia}(\delta_{jb}\delta_{kc} + \delta_{jc}\delta_{kb}) + \delta_{ib}(\delta_{ja}\delta_{kc} + \delta_{jc}\delta_{ka}) \\
& + \delta_{ic}(\delta_{ja}\delta_{kb} + \delta_{jb}\delta_{ka}), \\
(\Pi^S)^{a,b,c}_{i,i,i} = {} & 6\delta_{ia}\delta_{ib}\delta_{ic}, \\
(\Pi^S)^{a,a,a}_{i,j,k} = {} & 6\delta_{ia}\delta_{ja}\delta_{ka}, \\
(\Pi^S)^{a,b,b}_{i,j,k} = {} & 2\delta_{ia}\delta_{jb}\delta_{kb} + 2\delta_{ib}(\delta_{ja}\delta_{kb} + \delta_{jb}\delta_{ka}).
\end{aligned}$$

It is important to realize that with our choice of the independent parameters all triple Higgs couplings involving the singlet are proportional to λ or λ^2. This should not be the case for the coupling between three singlets, which gets contributions from S^3 and $|S^2|^2$ terms. In Eq. (2.35) this is proportional to $\lambda m_\kappa/\mu = \kappa$. The fact that this coupling exhibits a λ dependence is due to our choice of inputs m_κ and μ, which are more directly related to the mass of the singlino and the Higgsino; see Eq. (2.11).

B. Counting parameters and fields

Let us take stock and summarize the situation as regards the number of (physical) parameters and fields in the Higgs sector of the NMSSM. The physical scalar fields consist of three neutral CP-even Higgs bosons, h^0_1, h^0_2, h^0_3, two CP-odd Higgs bosons, A^0_1, A^0_2, and a charged Higgs boson, $H^\pm$. The NMSSM contains, of course, the SM gauge fields (and fermions). In particular, the SM gauge parameters

$$g, \quad g' \quad \text{and} \quad v = v_u^2 + v_d^2 \tag{2.37}$$

are traded for the following physical input parameters:

$$e, \quad M_W, \quad M_Z. \tag{2.38}$$

For these parameters we will apply the usual OS renormalization scheme. In particular, e will be defined in the Thomson limit. The Thomson limit, $q^2 \to 0$, may not be the most appropriate scale for the NMSSM processes whose loop corrections we will study; however, one can easily quantify the effect of using a running $\alpha_{\text{e.m.}}$ at the scale of the process. Besides these standard model parameters, the NMSSM introduces an additional set of nine parameters from the Higgs sector alone. From the Higgs potential, Eq. (2.4), it is clear that the Higgs sector of the NMSSM depends on the parameters,

$$\underbrace{t_\beta, \lambda, \kappa, \mu}_{\text{in } \tilde{\chi} \text{ sector also}}, \quad A_\lambda, \quad A_\kappa, \quad m_{H_d}, \quad m_{H_u}, \quad m_S, \tag{2.39}$$

where the first four parameters are also involved in the characterization of the neutralino/chargino sector, which we studied at length in the sister paper [44]. Alternatively

the last three soft Higgs masses can be traded for the tadpoles of the neutral Higgs which need to be constrained to zero to impose that the potential is at its minimum. The latter are therefore considered as physical observables,

$$\underbrace{t_\beta, \lambda, \kappa(m_\kappa), \mu,}_{\text{in } \tilde{\chi} \text{ sector also}} \qquad A_\lambda, \quad A_\kappa, \quad (\mathcal{T}_{H_d}, \mathcal{T}_{H_u}, \mathcal{T}_S). \tag{2.40}$$

The first six parameters above are not unambiguously defined in a simple mapping to an observable. We will discuss at length the choice and definitions of the input parameters that will construct the set of these six parameters. This issue is directly related to the renormalization scheme.

The parameters and fields of the neutralino/chargino sector were described in [44]. The parameters of this sector are the $U(1)$ and $SU(2)$ gaugino soft masses, M_1, M_2 in addition to t_β, λ, κ, μ.

III. RENORMALIZATION OF THE HIGGS SECTOR

A. A word about the gauge fixing

In this work we have restricted ourselves to the simplest gauge fixing; namely we take a linear gauge fixing constraint with a 't Hooft-Feynman parameter set to 1. Only the SM fields (including the necessary) Goldstone bosons appear, namely

$$\mathcal{L}_{\rm GF} = -|\partial^\mu W_\mu^+ + iM_W G^+|^2 - \frac{1}{2}\left|\partial^\mu Z_\mu^0 + i\frac{M_Z}{2}G^0\right|^2 - |\partial^\mu A_\mu|^2. \tag{3.1}$$

It is important to stress that all fields and parameters in Eq. (3.1) are understood to be *renormalized*.

B. Parameters, fields, and self-energies

What is also considered as renormalized are all the rotation matrices $U(\beta), P_a, S_h$. This is an approach we have consistently applied in all our work on the renormalization of supersymmetric models starting from the MSSM and imposed in all the sectors of the models where mixing between fields occurs, not only in the Higgs sector but also in the sfermion, neutralino, and chargino sectors [44–46]. In the MSSM a similar approach has also been considered for the chargino/neutralino [60] and sfermion [61] sectors. While one-loop corrections do reintroduce mixing, the use of wave function renormalization constants, with judicious choices of conditions imposed at scales corresponding to the physical masses of the particles, will ensure that even at one-loop transitions between particles with the same quantum numbers will vanish when these particles are on their mass shell.

With the exception of $\mathcal{L}_{\rm GF}, U(\beta), P_a$, and S_h all fields and parameters encountered so far are bare quantities. All bare quantities (X_0) are then decomposed into renormalized (X) and counterterms (δX) quantities. First, the SM parameters are shifted such that

$$g \to g + \delta g, \qquad g' \to g' + \delta g', \qquad v \to v + \delta v, \tag{3.2}$$

which are tantamount to

$$e \to e + \delta e, \quad M_W \to M_W + \delta M_W, \quad M_Z \to M_Z + \delta M_Z. \tag{3.3}$$

The same procedure applies to the NMSSM parameters in Eq. (2.39) or equivalently Eq. (2.40) with

$$\begin{aligned} t_\beta, \lambda, m_\kappa, \mu, A_\lambda, A_\kappa &\to t_\beta + \delta t_\beta, \lambda + \delta\lambda, m_\kappa + \delta m_\kappa, \\ &\quad \mu + \delta\mu, A_\lambda + \delta A_\lambda, A_\kappa + \delta A_\kappa, \\ \mathcal{T}_{H_d}, \mathcal{T}_{H_u}, \mathcal{T}_S &\to \mathcal{T}_{H_d} + \delta\mathcal{T}_{H_d}, \mathcal{T}_{H_u} \\ &\quad + \delta\mathcal{T}_{H_u}, \mathcal{T}_S + \mathcal{T}_S. \end{aligned} \tag{3.4}$$

For the fields all shifts are directly encoded in the wave function renormalization constants, so that mass eigenstates are expressed in terms of the current eigenstates in the same manner at one loop and at tree level. By current eigenstates we mean the states with definite electric charge, weak, and hypercharge quantum numbers before mixing occurs [see Eq. (2.5)] and diagonalization is performed. For the gauge fields we perform $W_\mu \to Z_W^{1/2} W_\mu$ while the system (A_μ, Z_μ^0) involves a matrix with four entries $\delta Z_{\gamma\gamma}, \delta Z_{\gamma Z}, \delta Z_{Z\gamma}, \delta Z_{ZZ}$ (see [62]). For the NMSSM Higgs sector, this entails that the three wave function renormalization matrices Z_S, Z_P, and Z_C, are introduced such that

$$\begin{aligned} \begin{pmatrix} h_1^0 \\ h_2^0 \\ h_3^0 \end{pmatrix}_0 &= Z_S^{1/2} \begin{pmatrix} h_1^0 \\ h_2^0 \\ h_3^0 \end{pmatrix}, \qquad \begin{pmatrix} G^0 \\ A_1^0 \\ A_2^0 \end{pmatrix}_0 = Z_P^{1/2} \begin{pmatrix} G^0 \\ A_1^0 \\ A_2^0 \end{pmatrix}, \\ \begin{pmatrix} G^\pm \\ H^\pm \end{pmatrix}_0 &= Z_C^{1/2} \begin{pmatrix} G^\pm \\ H^\pm \end{pmatrix}, \end{aligned} \tag{3.5}$$

where the index 0 is attached to the bare fields while the renormalized fields do not have an index. The elements of the wave function renormalization matrices can be written as

$$Z_C^{1/2} = \begin{pmatrix} 1 + \frac{1}{2}\delta Z_{G^\pm} & \frac{1}{2}\delta Z_{G^\pm H^\pm} \\ \frac{1}{2}\delta Z_{H^\pm G^\pm} & 1 + \frac{1}{2}\delta Z_{H^\pm} \end{pmatrix}, \tag{3.6}$$

$$Z_P^{1/2} = \begin{pmatrix} 1 + \frac{1}{2}\delta Z_{G^0} & \frac{1}{2}\delta Z_{G^0 A_1^0} & \frac{1}{2}\delta Z_{G^0 A_2^0} \\ \frac{1}{2}\delta Z_{A_1^0 G^0} & 1 + \frac{1}{2}\delta Z_{A_1^0} & \frac{1}{2}\delta Z_{A_1^0 A_2^0} \\ \frac{1}{2}\delta Z_{A_2 G^0} & \frac{1}{2}\delta Z_{A_2^0 A_1^0} & 1 + \frac{1}{2}\delta Z_{A_2^0} \end{pmatrix}, \tag{3.7}$$

$$Z_S^{1/2} = \begin{pmatrix} 1+\frac{1}{2}\delta Z_{h_1^0} & \frac{1}{2}\delta Z_{h_1^0 h_2^0} & \frac{1}{2}\delta Z_{h_1^0 h_3^0} \\ \frac{1}{2}\delta Z_{h_2^0 h_1^0} & 1+\frac{1}{2}\delta Z_{h_2^0} & \frac{1}{2}\delta Z_{h_2^0 h_3^0} \\ \frac{1}{2}\delta Z_{h_3^0 h_1^0} & \frac{1}{2}\delta Z_{h_3^0 h_2^0} & 1+\frac{1}{2}\delta Z_{h_3^0} \end{pmatrix}. \quad (3.8)$$

C. One-point functions and tadpoles

Once shifts on all parameters of the models including the tadpole terms [Eq. (3.4)] and wave function renormalization of the fields have been performed, we concentrate on the terms that are linear in the scalar fields and combine them with the one-loop contribution to these tadpoles. The tree-level condition on the tadpole is now elevated to the one-loop level so that minimization of the potential is realized. At one loop, the linear part of the potential can be written

$$V_{\rm lin}^{(1)} = (-\mathcal{T}_{h_d^0}^{\rm loop} + \delta\mathcal{T}_{h_d^0})\frac{h_d^0}{\sqrt{2}} + (-\mathcal{T}_{h_u^0}^{\rm loop} + \delta\mathcal{T}_{h_u^0})\frac{h_u^0}{\sqrt{2}} + (-\mathcal{T}_{h_s^0}^{\rm loop} + \delta\mathcal{T}_{h_s^0})\frac{h_s^0}{\sqrt{2}}, \quad (3.9)$$

where the first terms in the parentheses are the pure loop contributions and the second ones are the counterterms. We observe that because of the condition on the tree-level tadpoles, wave function renormalization of the Higgses does not enter. Our first renormalization condition is that these linear terms cancel. The loop contributions for the gauge eigenstates tadpoles are obtained from the mass eigenstates tadpoles with the use of the diagonalization matrix S_h,

$$\begin{pmatrix} \mathcal{T}_{h_d^0}^{\rm loop} \\ \mathcal{T}_{h_u^0}^{\rm loop} \\ \mathcal{T}_{h_s^0}^{\rm loop} \end{pmatrix} = S_h^{-1} \begin{pmatrix} \mathcal{T}_{h_1^0}^{\rm loop} \\ \mathcal{T}_{h_2^0}^{\rm loop} \\ \mathcal{T}_{h_3^0}^{\rm loop} \end{pmatrix}. \quad (3.10)$$

The minimum condition then gives simply

$$\delta\mathcal{T}_{h_i^0} = \mathcal{T}_{h_i^0}^{\rm loop}, \qquad i = d, u, s. \quad (3.11)$$

IV. BILINEARS AND TWO-POINT FUNCTION SELF-ENERGIES

A. Mass counterterms for the Higgs sector

We now turn to the bilinear terms in the Higgs fields and perform shifts in the parameters according to Eqs. (3.3) and (3.4). These shifts are performed on each of the underlying parameters (including the tadpoles) of the mass matrices $M_\pm^2, M_P^2, M_S^2$ in Eqs. (2.18), (2.22), (2.32). Since our approach is to use the same tree-level diagonalizing mass matrices, namely U_β, P_a, S_h, to convert to the physical fields, after the shifts the "physical" fields will now mix. Therefore apart from the induced diagonal counterterms $\delta M_{H^+}^2, \delta M_{A_{1,2}^0}^2, \delta M_{h_{1,2,3}^0}^2$, spurious counterterms to the Goldstones $\delta M_{G^0,G^\pm}^2$ are generated as well as nondiagonal mass mixings such as $\delta M_{h_1^0 h_2^0}^2$ and transitions such as $\delta M_{G^\pm H^\pm}^2$. Therefore, we need to enforce appropriate conditions to the one-loop wave function renormalization matrices such that a correct on-shell definition and normalization of the external particles is ensured. This is obtained by imposing that the residue of each (diagonal) propagator is equal to 1 (as is done in any theory without mixing). Strictly speaking, if we were only interested in having finite S-matrix elements and not finite Green's functions, wave function renormalization would not be a must. Still, the residues of the propagators of the external particles must be set to 1 to correctly normalize the S matrix, and this can be achieved by introducing finite wave function correction normalization factors to prevent nonvanishing transitions on the external legs.

Since the contributions of the tadpoles is very important, let us summarize how the shifts in the underlying parameters affect the mass matrices. Generically, in the bases d, u, s, the Higgs mass matrix M^2 [$M_\pm^2$ for the charged Higgs Eq. (2.18), M_P^2 for the pseudoscalars Eq. (2.22), and M_S^2 for the CP-even Higgses Eq. (2.32)] can be decomposed into a diagonal tadpole matrix T_M and a nontadpole matrix, which we denote M_M^2, such that

$$M^2 = T_M + M_M^2. \quad (4.1)$$

At tree level all T_M are set to zero, and the diagonalizing matrix U ($U = U_\beta, P_a, S_h$) is such that

$$M_D^2 = U M_M^2 U^{-1} \quad (4.2)$$

is diagonal with eigenvalues being the tree-level physical masses. In our notation, for the charged and pseudoscalar sectors the Goldstones are the (11) entries, and hence $(M_D)_{11} = 0$. The shifts entail the counterterm mass matrix

$$\delta M^2 = \delta T_M + \delta M_M^2. \quad (4.3)$$

In our approach, in all sectors of the NMSSM, to move to the (physical) basis $A_i^0, G_i^0, \ldots$ we use the *same matrix* as the one at tree level. From Eq. (4.3), the counterterm to this matrix is therefore

$$\delta M_{Ph}^2 = U\delta T_M U^{-1} + U\delta M_M^2 U^{-1} \quad (4.4)$$

(the subindex Ph generically denotes the mass matrix in the physical basis). In other words, M_{Ph}^2 is to be understood as being sandwiched between physical states $(A_i^0, G_i^0, \ldots)$. These are the mass counterterms that will be used to define the self-energies. In the code these counterterms are generated according to Eq. (4.4). As explained above due to these shifts δM_{Ph}^2 is no longer diagonal, and hence

the need for wave function renormalization is defined in such a way that when the physical states are on shell, no mixing occurs and the propagators have residue 1.

Equation (4.4) does not reveal some important properties of δM^2_{Ph}, especially that the matrices U do not necessarily have a simple analytic expression. In particular, we would like to emphasize that there are some simple algebraic expressions pertaining to the mixing between the Higgses and the Goldstones. These mixings will be needed when we write the important Ward identities between the Higgses and the gauge bosons in Sec. IV C. To arrive at a more transparent formula, it is more enlightening to express the above counterterms through the variation (counterterm) in M^2_D rather than M^2_M by using the relation for the mass eigenvalues according to Eq. (4.2) (note that there is no tadpole here). δM^2_D is a diagonal matrix that consists of the counterterms to the physical masses. Since M^2_D is a *function* of U and M_M, it is important to realize that shifts in M_D should be understood as shifts in *all parameters* that define M_D through Eq. (4.2) and in particular those entering U (and M_M). The fact that at this stage δU terms appear is not contrary to *the procedure* of using the same matrix U to move to the physical basis from the (u, d, s) basis. If an analytic formula for U in terms of all the underlying parameters existed, the variation/counterterm for all the elements of δU would correspond to taking the variation/counterterms for all these parameters. However, here, we do not need the exact analytic formula for U in terms of the underlying parameters; we will only exploit the unitarity of U, $\delta(U)U^{-1} + U\delta(U^{-1}) = 0$. Doing so we obtain

$$\begin{aligned}\delta M^2_{Ph} &= U\delta T_M U^{-1} + \delta M^2_D \\ &\quad + (U(\delta U^{-1})M^2_D + M^2_D(\delta U)U^{-1})), \\ (\delta M^2_{Ph})_{ij} &= (U\delta T_M U^{-1})_{ij} + (\delta M_D)^2_i\delta_{ij} \\ &\quad + (\delta(U)U^{-1})_{ij}((M_D)^2_i - (M_D)^2_j). \end{aligned} \tag{4.5}$$

Equation (4.5) shows that for the diagonal elements $(\delta M^2_{Ph})_{ii}$, the terms in δU vanish. As a special case, the counterterms to the Goldstones for both the charged and the pseudoscalar, δM^2_G (for $i = j = 1$), is a pure tadpole term as it should be. For the pseudoscalar case, we further exploit the important properties of P_a given in Eq. (2.31). We find that $\delta M^2_{G^\pm} = \delta M^2_{G^0}$. The mixing between a Goldstone and a non-Goldstone field is proportional to the (tree-level) mass of the associated non-Goldstone physical field. As stated at different occasions, because δM^2_{Ph} is no longer diagonal, Goldstone-Higgs mixing mass counterterms are generated and are given by the simple formulas for both the charged and pseudoscalar Higgses

$$\delta M^2_{H^\pm G^\mp} = \delta M^2_{G^\mp H^\pm} = \frac{s_{2\beta}}{2}\left(\delta T + M^2_{H^\pm}\frac{\delta t_\beta}{t_\beta}\right), \tag{4.6}$$

$$\delta M^2_{A^0_i G^0} = \delta M^2_{G^0 A^0_i} = \frac{s_{2\beta}}{2}\left(\delta T + M^2_{A^0_i}\frac{\delta t_\beta}{t_\beta}\right), \tag{4.7}$$

where

$$\delta T = \frac{1}{v s_{2\beta}}\sum_{i=1}^{3}(s_\beta S_{h,i1} - c_\beta S_{h,i2})\delta\mathcal{T}_{h^0_i}, \tag{4.8}$$

and the need for the wave function renormalization becomes evident in order to counterbalance the appearance of these transitions especially when the particles are on their mass shell.

B. Two-point functions from the Higgs potential

Implementing the wave function renormalization directly in the basis, we can write the renormalized self-energies, with the "non-hatted" expression as the result of the one-loop unrenormalized self-energy, while the δZ's are the result of the wave function renormalization. The mass shifts correspond exactly to the elements of δM^2_{Ph} (which include tadpoles). For the CP-even scalars we obtain $(i, j = 1, 2, 3)$

$$\begin{aligned}\hat{\Sigma}_{h^0_i h^0_j}(p^2) &= \Sigma_{h^0_i h^0_j}(p^2) + \delta M^2_{h^0_i h^0_j} - \frac{1}{2}(p^2 - M^2_{h^0_i})\delta Z_{h^0_i h^0_j} \\ &\quad - \frac{1}{2}(p^2 - M^2_{h^0_j})\delta Z_{h^0_j h^0_i}, \end{aligned} \tag{4.9}$$

while for the CP-odd scalars we get $(i, j = 1, 2)$

$$\begin{aligned}\hat{\Sigma}_{G^0G^0}(p^2) &= \Sigma_{G^0G^0}(p^2) + \delta M^2_{G^0} - p^2\delta Z_{G^0}, \\ \hat{\Sigma}_{A^0_i G^0}(p^2) &= \Sigma_{A^0_i G^0}(p^2) + \delta M^2_{A^0_i G^0} - \frac{1}{2}p^2\delta Z_{G^0 A^0_i} \\ &\quad - \frac{1}{2}(p^2 - M^2_{A^0_i})\delta Z_{A^0_i G^0}, \\ \hat{\Sigma}_{A^0_i A^0_j}(p^2) &= \Sigma_{A^0_i A^0_j}(p^2) + \delta M^2_{A^0_i A^0_j} - \frac{1}{2}(p^2 - M^2_{A^0_i})\delta Z_{A^0_i A^0_j} \\ &\quad - \frac{1}{2}(p^2 - M^2_{A^0_j})\delta Z_{A^0_j A^0_i}, \end{aligned} \tag{4.10}$$

and the charged scalars

$$\begin{aligned}\hat{\Sigma}_{G^\pm G^\pm}(p^2) &= \Sigma_{G^\pm G^\pm}(p^2) + \delta M^2_{G^\pm} - p^2\delta Z_{G^\pm}, \\ \hat{\Sigma}_{G^\pm H^\pm}(p^2) &= \Sigma_{G^\pm H^\pm}(p^2) + \delta M^2_{G^\pm H^\pm} - \frac{1}{2}p^2\delta Z_{G^\pm H^\pm} \\ &\quad - \frac{1}{2}(p^2 - M^2_{H^\pm})\delta Z_{H^\pm G^\pm}, \\ \hat{\Sigma}_{H^\pm H^\pm}(p^2) &= \Sigma_{H^\pm H^\pm}(p^2) + \delta M^2_{H^\pm} - (p^2 - M^2_{H^\pm})\delta Z_{H^\pm}. \end{aligned} \tag{4.11}$$

The aim now is to determine all the counterterms entering these expressions. Note that the Goldstones will mix, and we have singled out their appearance. Recall that

the Goldstone bosons are not physical; they cannot appear in initial or final states of a physical process. Thus, we do not need to renormalize their wave function, and we can set $\delta Z_{G^0} = \delta Z_{G^\pm} = 0$. Moreover, $\delta Z_{A_i^0 G^0}$ and $\delta Z_{H^\pm G^\pm}$ can also be set to 0 since they also correspond to transitions where a Goldstone boson is on an external leg.

C. $H^\pm W^\pm$ and $A^0_{1,2} Z^0$ transitions

At tree level the gauge fixing eliminates mixing between the gauge bosons and their corresponding Goldstone bosons therefore compensating for such a mixing that emerges from the gauge sector, $\mathcal{L}^{GV}$ (the gauge covariant kinetic term of the Higgs fields). We follow an approach where the gauge fixing is unrenormalized. As a result of shifting (both fields and parameters) in $\mathcal{L}^{GV}$, the massive gauge bosons and the pseudoscalars (as well as the Goldstones) will mix. Gauge invariance relates the gauge-pseudoscalar transitions and the corresponding Goldstones-pseudoscalar transition that we studied previously. Therefore we need to consider these transitions.

To get the remaining counterterms involving Goldstones, $\delta Z_{G^0 A_i^0}$ and $\delta Z_{G^\pm H^\pm}$, one also has to deal with new transitions between gauge bosons and CP-odd or charged Higgses. The expansion of the covariant derivative in the kinetic part of the scalar Lagrangian gives the following interaction terms:

$$\mathcal{L}^{GV} = M_Z(c_\beta \partial^\mu a_d^0 - s_\beta \partial^\mu a_u^0) Z_\mu^0 - M_W(i(c_\beta \partial^\mu h_d^- - s_\beta \partial^\mu h_u^-) W_\mu^+ + \text{H.c.}). \tag{4.12}$$

At tree level the combination of the scalar fields makes up the Goldstone bosons, the first component of the corresponding Higgs fields, namely

$$\begin{aligned} c_\beta a_d^0 - s_\beta a_u^0 &\equiv (P_a a^0)_1 = (\mathcal{P}^0)_1 = G^0, \\ c_\beta h_d^- - s_\beta h_u^- &\equiv (U(\beta) h^-)_1 = (\mathcal{H}^-)_1 = G^-. \end{aligned} \tag{4.13}$$

Take, for example, the case of the pseudoscalar/neutral Goldstones. Before applying the wave function renormalization, the shifts amount to

$$\begin{aligned} (P_a a^0)_1 \to ((\delta P_a) a^0)_1 &= ((\delta P_a) P_a^{-1} \mathcal{P}^0))_1 \\ &= ((\delta P_a) P_a^{-1})_{1i} (\mathcal{P}^0)_i. \end{aligned} \tag{4.14}$$

This shift alone, prior to wave function renormalization, will introduce $A_i^0 Z^0$ transitions, but not $G^0 Z^0$. This is easy to see. With $P_a = \hat{P}_a^{(3)} U(\beta)^{(3)}$ and using the fact that $(\hat{P}_a^{(3)})_{1i} = \delta_{1i}$ allows one to write

$$\begin{aligned} &\sum_{i=1}^{3} ((\delta P_a) P_a^{-1})_{1i} (\mathcal{P}^0)_i \\ &= -\sum_{i=1}^{2} A_i^0 \frac{s_{2\beta}}{2} (c_\beta P_{a,(i+1)2} + s_\beta P_{a,(i+1)1}) \frac{\delta t_\beta}{t_\beta} \\ &= -\sum_{i=1}^{2} A_i^0 \frac{s_{2\beta}}{2} \hat{P}_{a,i1} \frac{\delta t_\beta}{t_\beta}. \end{aligned} \tag{4.15}$$

Including the wave function renormalization, we obtain

$$\begin{aligned} \delta \mathcal{L}^{GV}_{\text{neutral}} = \frac{M_Z}{2} \Bigg\{ &\left(\delta Z_{ZZ} + \delta Z_{G^0} + \frac{\delta M_Z^2}{M_Z^2} \right) \partial^\mu G^0 Z_\mu^0 \\ &+ \delta Z_{Z\gamma} \partial^\mu G^0 A_\mu \\ &+ \sum_{i=1}^{2} \left(\delta Z_{G^0 A_i^0} - s_{2\beta} \hat{P}_{a,i1} \frac{\delta t_\beta}{t_\beta} \right) \partial^\mu A_i^0 Z_\mu^0 \Bigg\}. \end{aligned} \tag{4.16}$$

The first line of the equation above is the usual SM term. However, there remains nonvanishing transitions between pseudoscalars and the Z^0 boson, leading to the following self-energies:

$$\hat{\Sigma}_{A_i^0 Z^0}(p^2) = \Sigma_{A_i^0 Z^0}(p^2) + \frac{M_Z}{2} \left(\delta Z_{G^0 A_i^0} - s_{2\beta} \hat{P}_{a,i1} \frac{\delta t_\beta}{t_\beta} \right). \tag{4.17}$$

Following the same steps, the transition between the charged Higgs and the $W^\pm$ boson is given by

$$\hat{\Sigma}_{H^\pm W^\pm}(p^2) = \Sigma_{H^\pm W^\pm}(p^2) + \frac{M_W}{2} \left(\delta Z_{G^\pm H^\pm} - s_{2\beta} \frac{\delta t_\beta}{t_\beta} \right). \tag{4.18}$$

In the linear gauge we have used, there is a simple Ward identity that we derived in [45] starting from the Becchi-Rouet-Stora-Tyutin variation on the correlator between the Z-boson ghost and the pseudoscalar $\langle 0 | \bar{c}_Z(x) A_i^0(y) | 0 \rangle$. In the MSSM this identity was also formally set up at all orders in perturbation theory in [63]. The identity can readily be extended to the NMSSM using the unitarity properties of the matrix $\hat{P}_a$. This induces an identity that sets the following strong constraints:

$$\begin{aligned} &p^2 \hat{\Sigma}_{H^\pm W^\pm}(p^2) + M_{W^\pm} \hat{\Sigma}_{H^\pm G^\pm}(p^2) \\ &= -\frac{M_{W^\pm}}{2} (p^2 - M_{H^\pm}^2) \left(\delta Z_{H^\pm G^\pm} + s_{2\beta} \frac{\delta t_\beta}{t_\beta} - \mathcal{F}^\pm(p^2) \right), \\ &p^2 \hat{\Sigma}_{A_i^0 Z^0}(p^2) + M_{Z^0} \hat{\Sigma}_{A_i^0 G^0}(p^2) \\ &= -\frac{M_{Z^0}}{2} (p^2 - M_{A_i^0}^2) \left(\delta Z_{A_i^0 G^0} + s_{2\beta} \hat{P}_{a,i1} \frac{\delta t_\beta}{t_\beta} - \mathcal{F}^0(p^2) \right), \end{aligned}$$

where

$$\mathcal{F}^{\pm}(p^2) = \frac{\alpha}{8\pi s_W^2}\sum_{i=1}^{3}\left(c_{2\beta}S_{h,i1}S_{h,i2} + \frac{s_{2\beta}}{2}(S_{h,i2}^2 - S_{h,i1}^2)\right) \times B_0(p^2, M_W^2, M_{h_i^0}^2), \tag{4.19}$$

$$\mathcal{F}^{0}(p^2) = \frac{\alpha}{2\pi s_{2W}^2}\hat{P}_{a,i1}\sum_{i=1}^{3}\left(c_{2\beta}S_{h,i1}S_{h,i2} + \frac{s_{2\beta}}{2}(S_{h,i2}^2 - S_{h,i1}^2)\right)B_0(p^2, M_Z^2, M_{h_i^0}^2), \tag{4.20}$$

with $B_0(p^2, M_V^2, M_{h_i^0}^2)$ the scalar two point function [64] and $V = W, Z$.

The importance of these identities is that the $H^{\pm}G^{\pm}$ and $H^{\pm}W^{\pm}$ transitions (and their neutral counterparts) are not independent. In particular, we will be interested in setting an on-shell renormalization scheme whereby, on the mass shell, a transition between the charged Higgs and the charged Goldstone, and any of the neutral pseudoscalars and the neutral Goldstone boson, does not occur at one loop. In doing so, the identification that is made for these states at tree level is maintained. The previous identities show that at $p^2 = M_{H^{\pm}}^2$ and $p^2 = M_{A_i^0}^2$, transitions between these physical scalars and the corresponding gauge bosons do not occur either. It means that one can simultaneously set

$$\hat{\Sigma}_{H^{\pm}W^{\pm}}(M_{H^{\pm}}^2) = \hat{\Sigma}_{H^{\pm}G^{\pm}}(M_{H^{\pm}}^2) = 0,$$
$$\hat{\Sigma}_{A_i^0Z^0}(M_{A_i^0}^2) = \hat{\Sigma}_{A_i^0G^0}(M_{A_i^0}^2) = 0. \tag{4.21}$$

From Eqs (4.17), (4.18), and (4.21) we derive

$$\delta Z_{G^{\pm}H^{\pm}} = s_{2\beta}\frac{\delta t_\beta}{t_\beta} - \frac{2}{M_{W^{\pm}}}\Sigma_{H^{\pm}W^{\pm}}(M_{H^{\pm}}^2),$$
$$\delta Z_{G^0A_i^0} = s_{2\beta}\hat{P}_{a,i1}\frac{\delta t_\beta}{t_\beta} - \frac{2}{M_Z}\Sigma_{A_i^0Z^0}(M_{A_i^0}^2). \tag{4.22}$$

The Higgs masses that appear as arguments of the two-point function in the equations above are taken as the tree-level masses in order to be consistent with a fully one-loop treatment. These equations allow one to fix all wave function renormalization constants pertaining to the Goldstone bosons, and this will then leave us to deal with the system of the physical Higgses: the charged Higgs, the pair of pseudoscalars A_i^0, and the three CP-even neutral Higgses h_i^0. Likewise we deal with the gauge bosons whose renormalization goes now exactly the same way as the renormalization of the gauge sector within the SM. For the latter we follow the on-shell scheme adopted in [62]. Note that although this procedure permits us to decouple the Goldstones from the physical fields, to fully determine the values of $\delta Z_{G^{\pm}H^{\pm}}$ and $\delta Z_{G^0A_i^0}$ we still need to define a renormalization condition on δt_β. This will need an input from the physical Higgses to which we now turn.

D. Renormalization conditions from the Higgs self-energies

With the Goldstone bosons now set aside, the renormalized self-energies of the Higgses in Eqs. (4.9), (4.10), and (4.11) take the same form, allowing for one-loop transitions between them. Again, we require that the mixing between any two particles of the same CP parity must vanish at the mass of any physical particle (on-shell condition). The mass is defined as the pole mass of the real part of the renormalized inversed propagator. In case of mixing this requires solving a 3×3 (for the CP-even) and 2×2 (for the CP-odd) Higgs system of an inverse propagator. At one loop, these equations are linearized (see [45]). In this case, starting with a tree-level Higgs mass, $M_{i,\text{tree}}$ (i generically denotes $h_{1,2,3}^0, A_{1,2}^0, H^{\pm}$), the corrected one-loop mass is the solution of the equation

$$p^2 - M_{i,\text{tree}}^2 - \text{Re}\hat{\Sigma}_{ii}(p^2) = 0 \qquad p^2 = M_{i,1\,\text{loop}}^2, \tag{4.23}$$

which, in the one-loop approximation, reads

$$M_{i,1\,\text{loop}}^2 = M_{i,\text{tree}}^2 + \text{Re}\hat{\Sigma}_{ii}(M_{i,\text{tree}}^2) = M_{i,\text{tree}}^2 + \delta M_i^2 + \text{Re}\Sigma_{ii}(M_{i,\text{tree}}^2). \tag{4.24}$$

The above equation can be used in two ways. If all counterterms entering in δM_i^2 have been fixed (and hence are known), the above equation calculates the *finite* correction to the tree-level mass. The ultraviolet finiteness of the corrected mass is a very powerful check on the implementation of the one-loop setup. We may also use one or some of the masses of the Higgses as input parameters in order to solve for one or some of the counterterms to the underlying parameters that enter in δM_i^2. In this case

$$M_{i,1\,\text{loop}}^2 = M_{i,\text{tree}}^2 \equiv M_{i,\text{input}}^2 \to \delta M_i^2 = -\text{Re}\Sigma_{ii}(M_{i,\text{tree}}^2). \tag{4.25}$$

For instance, taking the charged Higgs mass $M_{H^{\pm}}$ as an input parameter gives

$$\delta M_H^{\pm} = -\Sigma_{H^{\pm}H^{\pm}}(M_{H^{\pm}}^2). \tag{4.26}$$

We also impose that the residue of the propagators for an on-shell physical field be equal to one such that

$$\text{Re}\hat{\Sigma}'_{ii}(M_{i,\text{tree}}^2) = 1 \quad \text{with} \quad \frac{\partial\hat{\Sigma}'_{ii}(p^2)}{\partial p^2} = \hat{\Sigma}'_{ii}(p^2), \tag{4.27}$$

which then fixes the diagonal entries of the wave function renormalization constants such that

$$\delta Z_i = \mathrm{Re}\Sigma'_{ii}(M^2_{i,\mathrm{tree}}) \quad (\text{for example}, \delta Z_{h^0_i} = \mathrm{Re}\Sigma'_{h^0_i h^0_i}(M^2_{h^0_i})). \tag{4.28}$$

We also impose that no mixing occurs between two same-parity fields when any of them is on shell. This condition translates into

$$\mathrm{Re}\hat{\Sigma}'_{ij}(M^2_{i,\mathrm{tree}}) = \mathrm{Re}\hat{\Sigma}'_{ij}(M^2_{j,\mathrm{tree}}) = 0 \quad \text{for } i \neq j, \tag{4.29}$$

which then fixes the nondiagonal elements of the wave function renormalization matrices such that

$$\delta Z_{ij} = 2\frac{\mathrm{Re}\Sigma_{ij}(M^2_{j,\mathrm{tree}}) + \delta M^2_{ij}}{M^2_{j,\mathrm{tree}} - M^2_{i,\mathrm{tree}}} \qquad i \neq j. \tag{4.30}$$

An example of the latter is

$$\delta Z_{h^0_i h^0_j} = 2\frac{\mathrm{Re}\Sigma_{h^0_i h^0_j}(M^2_{h^0_j}) + \delta M^2_{h^0_i h^0_j}}{M^2_{h^0_i} - M^2_{h^0_j}} \qquad i \neq j. \tag{4.31}$$

V. RENORMALIZATION SCHEMES

The definition of the underlying counterterms involves solving a system of coupled equations that, moreover, depends crucially on the choice of the input parameters, for example, which set of physical masses or other observables one chooses as input. In this respect, the wave function renormalization constants are somehow easy to evaluate. They involve a one-to-one relation and are independent from each other. Their expression is independent of the scheme.

We have also already specified; see Sec. II B for how the SM parameters, $g, g', v \leftrightarrow M_W, M_Z, e$ that enter also in the NMSSM, are renormalized.

The reconstruction of the counterterms of the nine underlying parameters of the Higgs sector in Eq. (2.40) is more complicated. Indeed, most of these parameters contribute to more than one Higgs mass (and chargino/neutralino mass) or Higgs observable. Apart from the tadpoles, defined from Eq. (3.11), it is not obvious what the optimal set of the nine input parameters should be in order to reconstruct these underlying parameters. Leaving the tadpole aside, there remain six parameters to determine in the Higgs sector. In principle, it is possible to use only masses as inputs since the Higgs sector does furnish six different Higgs masses, $h^0_{1,2,3}, A^0_{1,2}, H^\pm$. Technically, this requires the computation of the self-energies. Note that four of these parameters, t_β, λ, μ, κ, could also just as well be determined from the neutralino/chargino sector. However, as we argued in detail in [44], one cannot solve for the latter four parameters alone since the chargino/neutralino system involves also the underlying parameters M_1, M_2 [the $U(1)$ and $SU(2)$ gaugino soft masses]. The two parameters A_λ and A_κ can only be defined in the Higgs sector. The CP-even and CP-odd masses depend on both these parameters, while the charged Higgs mass depends on A_λ only. Because of the intrinsic interdependence of the NMSSM observables related to the Higgs sector (and the corresponding neutralino/chargino sector), in all generality we need to consider a system of counterterms for the eight underlying parameters that in a vector notation reads

$$\mathbb{p} = \Big(\underbrace{t_\beta, \lambda, \kappa(m_\kappa), \mu}_{\text{in } \tilde{\chi} \text{ and Higgs sectors}}, \underbrace{A_\lambda, A_\kappa}_{\text{Higgs}}, \underbrace{M_1, M_2}_{\tilde{\chi}}\Big), \tag{5.1}$$

for which we need to select eight input parameters with at least two from the chargino/neutralino sector and at least two from the Higgs system. Let us recall the procedure and the most important points that we detailed in [44] for reconstructing all eight counterterms. Injecting eight input parameters we have to solve for

$$\begin{pmatrix} \delta\mathtt{input}_1 \\ \cdots \\ \cdots \\ \delta\mathtt{input}_8 \end{pmatrix} = \mathcal{P}_{8,\mathrm{param}}\delta\mathbb{p} + \mathcal{R}_{8,\mathrm{residual}}, \tag{5.2}$$

where $\mathcal{P}_{8,\mathrm{param}}$ is an 8×8 matrix, and $\mathcal{R}_{\mathrm{n,residual}}$ contains other counterterms, such as gauge couplings, that are defined separately. Using the physical mass of one of the Higgs bosons as an input [see Eq. (4.26)] is a possible choice in an OS scheme. Not all inputs need to be OS. For an efficient resolution of Eq. (5.2), i.e., determining the $\delta\mathbb{p}$ vector, one should break up the connecting matrix $\mathcal{P}_{8,\mathrm{param}}$ into as many, possibly smallest rank, matrices as possible,

$$\mathcal{P}_{8,\mathrm{param}} = \mathcal{P}_{m,\mathrm{param}} \oplus \mathcal{P}_{p,\mathrm{param}} \oplus \cdots, \quad m + p + \cdots = 8. \tag{5.3}$$

The choice of the input parameters will determine how one can build the $\mathcal{P}_{8,\mathrm{param}}$ from smaller independent blocks, and each choice will define a renormalization scheme. It is important to seek a scheme where the determinant of each submatrix $\mathcal{P}_{p,\mathrm{param}}$ is not too small ($\delta\mathbb{p} \propto 1/\mathrm{Det}\mathcal{P}$) in order not to introduce large coefficients that would lead to large radiative corrections solely from a bad choice of inputs. We will pursue the comparisons between different schemes in the applications to Higgs decays in Sec. VIII.

A. Mixed OS-$\overline{\mathrm{DR}}$ schemes

Realizing that t_β is ubiquitous, it even enters the determination of the wave function renormalization matrices of the Higgses, a practical possibility is to take a $\overline{\mathrm{DR}}$ condition for t_β. In this case, the sectors for the Higgs, the

neutralinos, and the charginos can be solved independently. The counterterms for μ and the $SU(2)$ gaugino mass term M_2 can be extracted from both chargino masses. Then, the counterterms for the self-interacting singlet coupling κ (through m_κ), the $U(1)$ gaugino mass term M_1, and the singlet-doublet coupling λ can be obtained from the masses of the neutralinos that should be chosen to represent the mainly singlino, bino, and Higgsino neutralinos. We have commented at length about the issue of a *knowledge* of the nature (content) of the neutralinos in [44]. As concerns A_λ, A_κ, a possibility is, for example, to use both CP-odd Higgs bosons as inputs, $\delta M^2_{A^0_i} = \mathrm{Re}\Sigma_{A^0_i A^0_i}(M^2_{A^0_i})$, $i = 1, 2$. This breakup corresponds to

$$\mathcal{P}_{8,\mathrm{param}} = \underbrace{\mathcal{P}_{1,\mathrm{param}}}_{\overline{\mathrm{DR}},t_\beta} \oplus \underbrace{\mathcal{P}_{2,\mathrm{param}}}_{\mathrm{OS},M_{\chi^\pm_{1,2}}} \oplus \underbrace{\mathcal{P}_{3,\mathrm{param}}}_{\mathrm{OS},M_{\chi^0_{1,2,3}}} \oplus \underbrace{\mathcal{P}_{2,\mathrm{param}}}_{\mathrm{OS},M_{A^0_{1,2}}}. \tag{5.4}$$

The $\overline{\mathrm{DR}}$ condition for t_β in this scheme is an extension of the Dabelstein-Chankowski-Pokorski-Rosiek scheme [65–68], used in the context of the MSSM, to the NMSSM [25],

$$\frac{\delta t_\beta}{t_\beta} = \frac{1}{2}(\delta Z_{H_u} - \delta Z_{H_d})|_\infty, \tag{5.5}$$

where δZ_{H_u} and δZ_{H_d} are the wave function renormalization constants of the H_u and H_d doublets. The infinity symbol indicates that we only take the divergent part of the expression. δZ_{H_u} and δZ_{H_d} are related to the wave function renormalization constants $\delta Z_{h_i h_i}$ [Eqs. (3.8)] through

$$\begin{aligned}
\delta Z_{H_d} &= \frac{1}{R}\sum_{i,j,k=1}^{3} \epsilon_{ijk} S_{h,j3} S_{h,k2} \delta Z_{h_i h_i}, \\
\delta Z_{H_u} &= \frac{1}{R}\sum_{i,j,k=1}^{3} \epsilon_{ijk} S_{h,j1} S_{h,k3} \delta Z_{h_i h_i}, \\
R &= -\sum_{i,j,k=1}^{3} \epsilon_{ijk} S^2_{h_i 1} S^2_{h,j2} S^2_{h,k3},
\end{aligned} \tag{5.6}$$

where ϵ_{ijk} is the fully antisymmetric rank 3 tensor with $\epsilon_{123} = 1$.

In a $\overline{\mathrm{DR}}$ scheme only the divergent part of the counterterm is defined; i.e., any finite term is set to 0. Nonetheless, the scheme and the one-loop result is still not fully defined unless one specifies the renormalization scale $\bar{\mu}$. The latter is the remnant scale introduced by the regularization procedure, dimensional reduction. This class of renormalization schemes will be denoted as $t_{ijkA_1A_2}$. The letters i, j, k refer to the neutralinos whose mass has been taken as input. A_1A_2 is a reminder that the masses of the two physical pseudoscalars have also been used as input.

This disentangled scheme is rather simple to implement but can lead to a poor extraction of $\delta\lambda$, since this parameter is present only in nondiagonal entries of the neutralino mass matrix. A solution is to take another Higgs mass as input to get this counterterm, but in this case the neutralino and the Higgs sectors are no longer disassociated.

B. Fully on-shell schemes

For these schemes, the set of eight counterterms, including t_β, are obtained from OS conditions based on inputs taken from physical masses. As for the previous scheme, $\delta\mu$ and δM_2 will mainly be reconstructed from the two chargino masses but not fully since there is still some mixing introduced by t_β. In addition, it is natural to take the neutralino that is mainly bino to extract δM_1. The parameters $\delta\lambda$ and δm_κ can be extracted from either the neutralino or the Higgs sector. As before, δA_λ and δA_κ have to be extracted from two masses from the Higgs sector including at least a mostly singlet Higgs. Finally, it is much better to obtain δt_β from an additional Higgs input than from the neutralino masses, as was shown in [44]. We are then left with a system of eight equations, whose inversion will give all these counterterms.

Different classes of such (fully) on-shell renormalization schemes are possible. For instance, one can take one example from the general class where the masses of the two charginos are exploited. This furnishes a system of two equations. One can then have variations on this scheme depending on which source provides the other parameters.

(i) One scheme could use the masses of three neutralinos as well as the masses of both pseudoscalar Higgses and the mass of the charged Higgs. This choice is referred to as $\mathrm{OS}_{ijkA_1A_2H^+}$ where $i, j, k = 1, \ldots, 5$ designates the three chosen neutralinos, usually a bino, a singlino, and a Higgsino.

(ii) Another choice could be based on the masses of (only) two neutralinos, both pseudoscalar Higgses, the charged Higgs, and an additional CP-even Higgs different from the SM-like Higgs. This subclass is labeled as $\mathrm{OS}_{ijh_{\hat{i}}A_1A_2H^+}$ where $i, j = 1, \ldots, 5$ and $\hat{\imath} = 1, 2, 3$.

(iii) The third possibility is to use the mass of one neutralino, the bino, and the masses of five Higgses, in the obvious notation, $\mathrm{OS}_{ih_{\hat{i}}h_{\hat{j}}A_1A_2H^+}$ where $i = 1, \ldots, 5$ and $\hat{\imath}, \hat{\jmath} = 1, 2, 3$.

The numerical examples we will consider are based on the $\mathrm{OS}_{ijh_{\hat{i}}A_1A_2H^+}$ with an optimal choice for the neutralinos.

VI. CHECKS ON THE RESULTS AND TRACKING THE SCHEME DEPENDENCE

To check the validity of our numerical results, we perform several tests. The most powerful test consists in checking the absence of ultraviolet divergences on all the observables that we calculate. Ultraviolet divergences appear in many intermediate steps of the calculations and get canceled out by the counterterms for the underlying parameters and/or among many diagrams. The ultraviolet

divergences are encoded in the parameter $C_{\rm UV}$ defined in dimensional reduction as $C_{\rm UV} = 2/\epsilon - \gamma_E + \ln(4\pi)$ where $\epsilon = 4 - d$ (d being the number of dimensions) and γ_E is the Euler constant. We systematically check that the numerical results, for one-loop corrections to masses or to decay processes, are independent of $C_{\rm UV}$ by varying this parameter from 0 to 10^7. We require that the numerical results agree for at least seven digits (SloopS uses double precision). Thus we ensure that physical processes are finite for all renormalization schemes.

Finally, in schemes where at least one parameter is taken to be $\overline{\rm DR}$, a dependence on the renormalization scale $\bar{\mu}$ remains, this can be used to quantify the scale dependence.

A. The β functions and the scale dependence

In order to gain a qualitative understanding of the differences in the results for the one-loop corrections to the decay processes we have studied in different schemes, it is interesting to recall some simple arguments related to the counterterms. The infinite ($C_{\rm UV}$) part of any counterterm is obviously the same regardless of the renormalization scheme, and this is one of the reasons our checks show finiteness for the calculated observable for all schemes. The finite part of the counterterm is, however, scheme dependent. The difference in this finite part for a particular parameter can be large between two schemes. This difference may get amplified in the computation of an observable that depends strongly on this particular parameter. This parametric dependence that can be derived from the study of the observable at tree level is therefore an important ingredient also. Take a parameter $\mathbb{p}_i$, and its counterterm, within some scheme $Q_{\mathbb{p}_i}$, reads

$$\delta\mathbb{p}_i/\mathbb{p}_i = \beta_{\mathbb{p}_i}(C_{\rm UV} + \ln(\bar{\mu}^2/Q^2_{\mathbb{p}_i})). \tag{6.1}$$

$\bar{\mu}$ is the scale introduced by dimensional reduction. $\beta_{\mathbb{p}_i}$ as defined here is the one-loop β constant for the parameter $\mathbb{p}_i$. It is scheme independent. $Q^2_{\mathbb{p}_i}$ encodes the scheme dependence. In this notation, different schemes correspond to different values of $Q^2_{\mathbb{p}_i}$. $Q^2_{\mathbb{p}_i}$ is the square of some mass scale that represents both external momenta (corresponding to the choice of the subtraction points) and internal masses typical of two-point functions. All our renormalization schemes are based on two-point functions. If $Q^2_{\mathbb{p}_i}$ is dominated by a mass m_P much larger than all other scales in the problem, then $Q_{\mathbb{p}_i} \sim m_P$. Note, however, that these two-point functions can also involve nonlog constant terms; in our definition these nonlog terms are lumped into $Q_{\mathbb{p}_i}$. Within the same scheme, $Q^2_{\mathbb{p}_i}$, the difference in the value of the counterterm due to a change in the regularization scale $\bar{\mu}$ is a measure of $\beta_{\mathbb{p}_i}$,

$$\Delta_{\mu_2-\mu_1}\delta\mathbb{p}_i/\mathbb{p}_i = \delta\mathbb{p}_i(\bar{\mu}_2)/\mathbb{p}_i - \delta\mathbb{p}_i(\bar{\mu}_1)/\mathbb{p}_i = \beta_{\mathbb{p}_i}\ln(\bar{\mu}_2^2/\bar{\mu}_1^2). \tag{6.2}$$

In our code this is how we determine $\beta_{\mathbb{p}_i}$ numerically. In our numerical analysis in Sec. VIII these β constants have been checked against the β functions given in [4]. Perfect agreement has been found when specializing to the one-loop result. This is a nontrivial check on our renormalization procedure. For the so-called $\overline{\rm DR}$ scheme, we set the corresponding counterterm to

$$\delta^{\overline{\rm DR}}\mathbb{p}_i/\mathbb{p}_i = \beta_{\mathbb{p}_i}C_{\rm UV}, \tag{6.3}$$

which in effect corresponds to choosing a scale $Q_{\mathbb{p}_i} = \bar{\mu}$.

The one-loop correction to an observable involves calculating all the virtual two-point, three-point, …, n-point functions that are specific for a given amplitude (regardless of the scheme) and then including the counterterms for all parameters on which the amplitude $\mathcal{O}$ depends to obtain a finite result. The dependence of the amplitude on a specific parameter $\mathbb{p}_i$, the parametric dependence alluded to earlier, is obviously also very important. If at tree level we slightly change the value of the parameter $\mathbb{p}_i$ by an amount $\delta\mathbb{p}_i$, we define the percentage change on the observable as

$$\frac{\delta\mathcal{O}}{\mathcal{O}} = \sum_i \kappa_{\mathbb{p}_i}\frac{\delta\mathbb{p}_i}{\mathbb{p}_i}. \tag{6.4}$$

The sum is over all the *independent* parameters of the model. If an observable is independent of a particular parameter $\mathbb{p}_i$, then the corresponding $\kappa_{\mathbb{p}_i}$ is $\kappa_{\mathbb{p}_i} = 0$.[1] In this definition of the parametric dependence we are assuming small, infinitesimal, $\delta\mathbb{p}_i$ as is generally the case when $\delta\mathbb{p}_i$ stand for one-loop counterterms or else that the dependence in the parameter $\mathbb{p}_i$ is linear. With this proviso and to make the discussion simple, if all counterterms are defined on shell, or at some subtraction point according to Eq. (6.1), then the virtual corrections for the amplitude can be written in a very compact way as

$$\delta\mathcal{O}^{\rm OS}/\mathcal{O} = \sum_i \beta_{\mathbb{p}_i}\kappa_{\mathbb{p}_i}\ln(Q^2_\Delta/Q^2_{\mathbb{p}_i}). \tag{6.5}$$

The correction can be large if some β constants are large. The corrections could also be amplified if the parametric dependence on the parameter $\kappa_{\mathbb{p}_i}$ is large and/or if there is a large difference between some subtraction scale in defining a particular parameter, namely $Q^2_{\mathbb{p}_i}$ and the scale that defines the observable Q_Δ. Q_Δ can have contributions not only from two-point functions but also from n-point functions that we have lumped in its definition. In particular, our parametrization of Q_Δ can take into account nonsingle logarithms (dilogarithms,…). In particular, some

[1]Strictly speaking the sum applies to each Lorentz structure and/or helicity amplitude.

TABLE I. Parameters for the benchmark Point A (in GeV for all dimensionful parameters). $Q_{\rm susy}$ is calculated as $Q_{\rm susy} = \sqrt{M_{\tilde{t}_1} M_{\tilde{t}_2}} = 1117.25$ GeV. The derived values for the tree-level masses of all Higgses, charginos, and neutralinos are also given. For this benchmark, the top mass, crucial for the computation of the Higgs mass in particular, is taken as $M_t = 175$ GeV.

M_1	700	λ	0.1	A_κ	0	$m_{\tilde{Q}_3}$	1740	$m_{\tilde{D},\tilde{U}_{1,2}}$	1000
M_2	1000	m_κ (κ)	120 (0.1)	A_t	4000	$m_{\tilde{U}_3}$	800	$m_{\tilde{L}_3}$	1000
M_3	1000	μ	120	A_b	1000	$m_{\tilde{D}_3}$	1000	$m_{\tilde{l}_3}$	1000
t_β	10	A_λ	150	A_l	1000	$m_{\tilde{Q}_{1,2}}$	1000	$m_{\tilde{L},\tilde{l}_{1,2}}$	1000

$(M_{\chi_1^+}, M_{\chi_2^+}; M_{\tilde{\chi}_1^0}, M_{\chi_2^0}, M_{\tilde{\chi}_3^0}, M_{\tilde{\chi}_4^0}, M_{\chi_5^0}) = (117.95, 1006.61; 112.77, 123.80, 241.57, 702.82, 1006.64)$ $(M_{H^\pm}; M_{A_1^0}, M_{A_2^0}; M_{h_1^0}, M_{h_2^0}, M_{h_3^0}) = (577.33; 12.64, 572.06; 88.47, 240.07, 572.48)$. The one-loop corrected SM-like Higgs mass is calculated to be 125.45 GeV in the $\mathrm{OS}_{34h_2A_1A_2H^+}$ and 126.47 GeV in the $\overline{\rm DR}$ scheme with a scale at $Q_{\rm susy}$. This difference is solely due to the scheme dependence.

one-loop dynamics may entail large genuine corrections that are then translated here as large values of Q_Δ.

In a scheme where *all* counterterms are defined *à la* $\overline{\rm DR}$,

$$\delta\mathcal{O}^{\overline{\rm DR}}/\mathcal{O} = \ln(Q_\Delta^2/\bar{\mu}^2)\sum_i \beta_{\mathbb{p}_i}\kappa_{\mathbb{p}_i}. \tag{6.6}$$

There is now a scale dependence that quantifies the uncertainty in the one-loop calculation. The correction is minimized for $\bar{\mu} \sim Q_\Delta$. Again if the virtual corrections are dominated by single logs with an argument corresponding to the largest scale/mass of the process, the corrections are minimized for $\bar{\mu}$ corresponding to this highest scale.

In a mixed scheme such as the one we have taken with $\mathbb{p}_0 = t_\beta$ and with $Q_{\mathbb{p}_0}$ the effective scale that defines the OS definition of t_β, the result for the correction to the same observable can be written as[2]

$$\delta\mathcal{O}^{\rm mixed}/\mathcal{O} = \delta\mathcal{O}^{\rm OS}/\mathcal{O} + \beta_{\mathbb{p}_0}\kappa_{\mathbb{p}_0}\ln(Q_{\mathbb{p}_0}^2/\bar{\mu}^2). \tag{6.7}$$

The β functions can also be derived from an analysis of the renormalization group. The system of coupled equations at two loop is given in [4]. Specializing to one loop and keeping only the dominant Yukawa coupling contributions, the system is rather simple and can help understand some features of the full one-loop calculation. With h_t the top-Yukawa coupling, the dominant contributions to the running of the underlying couplings of the NMSSM, can be cast as

$$\frac{1}{h_t^2}\frac{\mathrm{d}h_t^2}{\mathrm{d}\tau} = \frac{1}{A_t}\frac{\mathrm{d}A_t}{\mathrm{d}\tau} = \frac{2}{\lambda^2}\frac{\mathrm{d}\lambda^2}{\mathrm{d}\tau} = \frac{2}{\mu^2}\frac{\mathrm{d}\mu^2}{\mathrm{d}\tau} = 6h_t^2 \quad \text{and}$$
$$\frac{1}{A_\lambda}\frac{\mathrm{d}A_\lambda}{\mathrm{d}\tau} = 3h_t^2\frac{A_t}{A_\lambda}, \tag{6.8}$$

with $\tau = \ln\bar{\mu}^2/16\pi^2$. What this shows is that if $A_t \gg A_\lambda$, then β_{A_λ} can be quite large. Remember that a large A_t is needed for inducing a large one-loop correction to the MSSM-like *CP*-even Higgs (in the MSSM limit). Note that A_κ and $s = \mu/\lambda$ do not have top-Yukawa enhanced running.

B. Infrared divergences

Many of the Higgs processes we will study at the one-loop level, will give rise to infrared divergences when electrically charged particles are involved in the external legs. The treatment of these divergences requires the computation of real photon emission as described in [44]. In a nutshell, for these $1 \to 2$ decays it is sufficient to take an infinitesimally small photon mass as a regulator. For more details see [44].

VII. THE BENCHMARK POINTS

We will concentrate on two quite distinct scenarios of the NMSSM. The first scenario, Point A, is chosen with a very small value of the mixing parameter λ in order to study the MSSM limit. Point B has a much larger value of λ exhibiting large mixing between the singlet and doublet components.

Point A is defined through practically the same parameters that we chose to set the benchmark Point 3 in our previous work [44] on the renormalization of the chargino/neutralino sector. The defining parameters of Point A are listed in Table I. An alert reader would have noticed that the difference between Point 3 in [44] and Point A is that the values of the stop masses were modified to ensure that the one-loop corrected mass for the SM-like Higgs would be compatible with the value observed at the LHC. Because of the small value of λ, we are in the MSSM limit, which requires us to take a fairly large value of the trilinear parameter, A_t, in the stop sector. Observe that the value of A_t is very large compared to A_λ with $A_t/A_\lambda \sim 27$. This will have important side effects apart from giving large corrections to the lightest *CP*-even neutral Higgs. We have also listed the value of the one-loop corrected mass for the SM-like Higgs. We see that it is compatible with the mass of the Higgs discovered at the LHC. Table I gives the value of this

[2]In a scheme where all parameters are defined on shell according to Eq. (6.1), the numerical extraction of the β constants through the μ variation is quite simple, it relies on the combination $(C_{\rm UV} + \ln\bar{\mu}^2)$. In a mixed scheme such as the one where t_β is $\overline{\rm DR}$ and the other underlying parameters are reconstructed from solving a coupled system based on on-shell quantities through masses as input, there may be a mismatch between the coefficient multiplying $C_{\rm UV}$ and $\ln\bar{\mu}^2$.

TABLE II. Parameters for the benchmark Point B (in GeV for all dimensionful parameters). $Q_{\rm susy}$ is calculated as $Q_{\rm susy} = \sqrt{M_{\tilde{t}_1} M_{\tilde{t}_2}} = 753.55$ GeV. The derived values for the tree-level masses of all Higgses, charginos, and neutralinos are also given.

M_1	120	λ	0.67	A_κ	0	$m_{\tilde{Q}_3}$	750	$m_{\tilde{D},\tilde{U}_{1,2}}$	1500
M_2	300	m_κ (κ)	59.7 (0.2)	A_t	1000	$m_{\tilde{U}_3}$	750	$m_{\tilde{L}_3}$	1500
M_3	1500	μ	200	A_b	1000	$m_{\tilde{D}_3}$	1500	$m_{\tilde{l}_3}$	1500
t_β	1.92	A_λ	405	A_l	1000	$m_{\tilde{Q}_{1,2}}$	1500	$m_{\tilde{L},\tilde{l}_{1,2}}$	1500

$(M_{\chi_1^+}, M_{\chi_2^+}; M_{\tilde{\chi}_1^0}, M_{\chi_2^0}, M_{\tilde{\chi}_3^0}, M_{\tilde{\chi}_4^0}, M_{\chi_5^0}) = (159.63, 342.70; 89.99, 143.90, 196.18, 235.64, 344.98)$ $(M_{H^\pm}; M_{A_1^0}, M_{A_2^0}; M_{h_1^0}, M_{h_2^0}, M_{h_3^0}) = (469.09; 111.59, 481.56; 102.92, 142.84, 479.00)$. The one-loop corrected SM-like Higgs mass is calculated to be 124.44 GeV in the $\mathrm{OS}_{12h_2A_1A_2H^+}$ and 121.62 GeV in the $\overline{\rm DR}$ scheme with a scale at $Q_{\rm susy}$. To calculate the Higgs mass we have taken a running top mass at the scale $Q_{\rm susy} = \sqrt{M_{\tilde{t}_1} M_{\tilde{t}_2}}$ with $M_t = 146.94$ GeV. This difference is solely due to the scheme dependence.

mass in two schemes. The scheme difference is within 1 GeV. For more details on the correction to the Higgs masses and tuned comparisons with other calculations we refer to [69].

For the second benchmark, we borrowed parameters very similar to Point TP4 in [69]. Benchmark B is defined in Table II.

One notable difference between the two benchmark points is the value of λ (6 times larger for Point B), such that for Point B, $\Lambda_v > M_Z$. As a consequence, for Point B the tree-level value for the mass of the SM-like Higgs is larger than M_Z, which is not the case for Point A. This is the reason why for Point B the value of t_β is ~ 2 and more importantly $A_t/A_\lambda \sim 2.5$ only. Still, one needs radiative corrections to lift the mass of the SM-like Higgs from 103 GeV at tree level to about 125 GeV.

Because we will study Higgs decays either to other Higgses or to neutralinos and charginos, the field content (in terms of the current, unmixed, fields) is very important. The field content or the purity of the physical fields, at tree level, is given in Table III. If we arrange the physical fields in terms of their dominant component, then for

Point A

$$(\tilde{\chi}_1^0, \tilde{\chi}_2^0, \tilde{\chi}_3^0, \tilde{\chi}_4^0, \tilde{\chi}_5^0; \tilde{\chi}_1^+, \tilde{\chi}_2^+) \sim (\tilde{H}^0, \tilde{H}^0, \tilde{S}^0, \tilde{B}^0, \tilde{W}_3^0; \tilde{H}^+, \tilde{W}^+),$$
$$(h_1^0, h_2^0, h_3^0; A_1^0, A_2^0) \sim (h_u^0, h_s^0, h_d^0; a_s^0, a_d^0). \quad (7.1)$$

For Point A the states have a very high degree of purity. Given the fact that $\tilde{\chi}_1^0$ is mostly Higgsino, $\tilde{\chi}_3^0$ is mostly singlino, and $\tilde{\chi}_4^0$ mostly bino, this justifies the use of the $t_{134A_1A_2}$ mixed OS-$\overline{\rm DR}$ renormalization scheme, following the notation of Sec. V A, and the $\mathrm{OS}_{34h_2A_1A_2H+}$ renormalization scheme, following the notation of Sec. V B, to compute the one-loop corrections. Indeed, as discussed in [44], in choosing the input masses, one should preferably include the bino and singlino from the neutralino sector, and the Higgsino when a third neutralino is to be used.

For Point B, there is strong mixing and only the lightest physical pseudoscalar field can be described as pure; nonetheless, we can write the dominant components,

TABLE III. Components of the mass eigenstates for benchmark Points A and B. The dominant component is highlighted.

		Point A	Point B
h_1^0	h_d^0	1.1%	22.5%
	h_u^0	**98.6%**	**67.4%**
	h_s^0	0.3%	10.1%
h_2^0	h_d^0	0.1%	0.%
	h_u^0	0.3%	12.5%
	h_s^0	**99.6%**	**87.5%**
h_3^0	h_d^0	**98.8%**	**77.5%**
	h_u^0	1.1%	19.7%
	h_s^0	0.1%	2.8%
A_1^0	a_d^0	0%	1.8%
	a_u^0	0%	0.5%
	a_s^0	**100%**	**97.7%**
A_2^0	a_d^0	**99.0%**	**76.9%**
	a_u^0	1.0%	20.8%
	a_s^0	0.0%	2.3%
$\tilde{\chi}_1^0$	$\tilde{B}^0$	...	**56.6%**
	$\tilde{W}^0$	...	32.3%
	$\tilde{h}^0$	**98.4%**	10.3%
	$\tilde{S}^0$	0.77%	0.8%
$\tilde{\chi}_2^0$	$\tilde{B}^0$	...	4.0%
	$\tilde{W}^0$	...	2.6%
	$\tilde{h}^0$	**99.5%**	19.3%
	$\tilde{S}^0$	...	**74.0%**
$\tilde{\chi}_3^0$	$\tilde{B}^0$	...	10.1%
	$\tilde{W}^0$	...	...
	$\tilde{h}^0$	0.9%	**78.9%**
	$\tilde{S}^0$	**99.1%**	11.0%
$\tilde{\chi}_4^0$	$\tilde{B}^0$	**99.6%**	18.1%
	$\tilde{W}^0$	...	12.3%
	$\tilde{h}^0$	...	**55.8%**
	$\tilde{S}^0$	...	13.7%
$\tilde{\chi}_5^0$	$\tilde{B}^0$	...	11.2%
	$\tilde{W}^0$	**99.3%**	**52.8%**
	$\tilde{h}^0$	0.69%	35.7%
	$\tilde{S}^0$	...	0.4%

Point B

$$(\tilde{\chi}_1^0,\tilde{\chi}_2^0,\tilde{\chi}_3^0,\tilde{\chi}_4^0,\tilde{\chi}_5^0;\tilde{\chi}_1^+,\tilde{\chi}_2^+) \sim (\tilde{B}^0,\tilde{S}^0,\tilde{H}^0,\tilde{H}^0,\tilde{W}_3^0;\tilde{H}^+,\tilde{W}^+),$$
$$(h_1^0,h_2^0,h_3^0;A_1^0,A_2^0) \sim (h_u^0,h_s^0,h_d^0;a_s^0,a_d^0). \quad (7.2)$$

We will therefore use the $t_{123A_1A_2}$ and $\mathrm{OS}_{12h_2A_1A_2H+}$ renormalization schemes to compute the radiative corrections.

VIII. HIGGS DECAYS

As an application to our setup for the renormalization of the Higgs sector and its implementation in SloopS we consider Higgs decays. This covers decays of Higgses into neutralinos and charginos, final states with a single gauge boson, as well as decays into lighter Higgses. These channels also serve to test the most critical aspects of the renormalization of the Higgs sector in the NMSSM. We have not computed decays involving sfermions since the sfermion sector does not introduce much novelty compared to the MSSM, nor did we consider here decays into SM fermions and pairs of gauge bosons. Note that we have computed decays of the neutral Higgs scalars to $\gamma\gamma$ and $Z\gamma$ in an earlier publication [59]; however, these loop induced decays do not require renormalization.

The importance of the radiative corrections and the choice of the renormalization scheme underline the importance of studying the parametric dependence. To gain an understanding, at least qualitatively, of the results of some of the radiative corrections for the most prominent decays of the Higgses, we will first show, for both Points A and B, how the value of the corresponding *tree-level* partial width changes when one of the underlying parameters is modified around each one of the reference points that define the model. As discussed in Sec. VI A this will give us an insight on the parametric dependence and an approximate extraction of the coefficients $\kappa_{\mathbb{p}_i}$ (see Eq. (6.4) when specializing to small variations. We will, in fact, only show the variations of the square of the coupling involved in the decay. This quantity represents the square of the amplitude for the partial width, leaving the phase space factor out. The rationale for doing this is that a variation of the underlying parameters changes also the values of the masses, which in turn change the phase space and hence introduce another source of change in the partial width. In the renormalization process some of the masses of the particles taking part in the process are taken as input parameters with a value fixed at all orders.

Before giving the results for the full one-loop corrections to the decays, we will first extract the universal $\beta_{\mathbb{p}_i}$ for each parameter $\mathbb{p}_i$ as explained in Sec. VI A. For each scheme we will also give the value of the finite term [see Eq. (6.1)] of the counterterm to the parameter $\mathbb{p}_i$,

$$\left.\frac{\delta\mathbb{p}_i}{\mathbb{p}_i}\right|_{\text{finite}} = \beta_{\mathbb{p}_i}\ln(\bar{\mu}^2/Q_{\mathbb{p}_i}^2), \quad (8.1)$$

evaluated at a value of $\bar{\mu}$ that we will specify. For later reference, observe that a large value of $\beta_{\mathbb{p}_i}$ will most certainly entail a large value for the finite part of the corresponding counterterm, unless $\bar{\mu}^2 \sim Q_{\mathbb{p}_i}^2$. Remembering our discussion in Sec. VI A [see also Eqs. (6.5) and (6.6)], the $\beta_{\mathbb{p}_i}$ and the finite part of the counterterms in a given scheme, together with what we will have learned about the parametric dependence, will help gain some understanding of the results of the full one-loop corrections, the scheme dependence. One could also learn whether there may be large genuine corrections that stem from the two- and three-point functions or even from the real corrections (bremmstrahlung).

A. Point A

For this point we will compute the full electroweak corrections to the partial decay widths of *CP*-even, *CP*-odd, and charged Higgs into other Higgses and supersymmetric particles. For the latter, only neutralinos and charginos are kinematically accessible. We will only include the channels for which the branching ratio is above 1% as they are the only potentially relevant ones. Note that the lightest *CP*-even and *CP*-odd Higgs decay only into SM particles and that the components of the heavy doublet Higgs (h_3^0, A_2^0) also decay mainly into SM particles, in particular $b\bar{b}$. Only the singlet h_2^0 decays dominantly in the pair of singlets $A_1^0A_1^0$. The partial widths of all the channels considered are of the same order at tree level, about 10^{-2} GeV.

1. Tree level. Parameter dependence on some couplings in Higgs decays

As promised, and before going to the loop results, we first look at the parametric dependence of some of the decays we will study. The analysis of the parametric dependence relies on the tree-level behavior of the observables as the underlying parameters are varied. Results of these variations are shown in Fig. 1. The first general observation is the smooth and almost linear dependence on all the (independent) parameters, for all the coupling across the whole range of the variations, ±20%. This can easily be understood if we recall that this point is characterized by very small mixing λ where the physical states have a high degree of purity, whereby the Higgs states h_2^0, A_1^0 and the neutralino χ_3^0 are essentially singlet states. With this small λ scenario, it is instructive to subdivide these decays into three classes of decays

(i) All particles involved in the decay are predominantly singlets, $h_2^0 \to A_1^0A_1^0$.
(ii) None of the particle taking part in the decay is singletlike with characteristics close to the MSSM and with very little dependence on λ. Two examples are shown in Fig. 1, $A_2^0 \to \tilde{\chi}_1^+\tilde{\chi}_1^-$ and $A_2^0 \to \tilde{\chi}_1^0\tilde{\chi}_1^0$. In the one-loop calculation we will also consider $h_3^0 \to \tilde{\chi}_1^+\tilde{\chi}_1^-$.

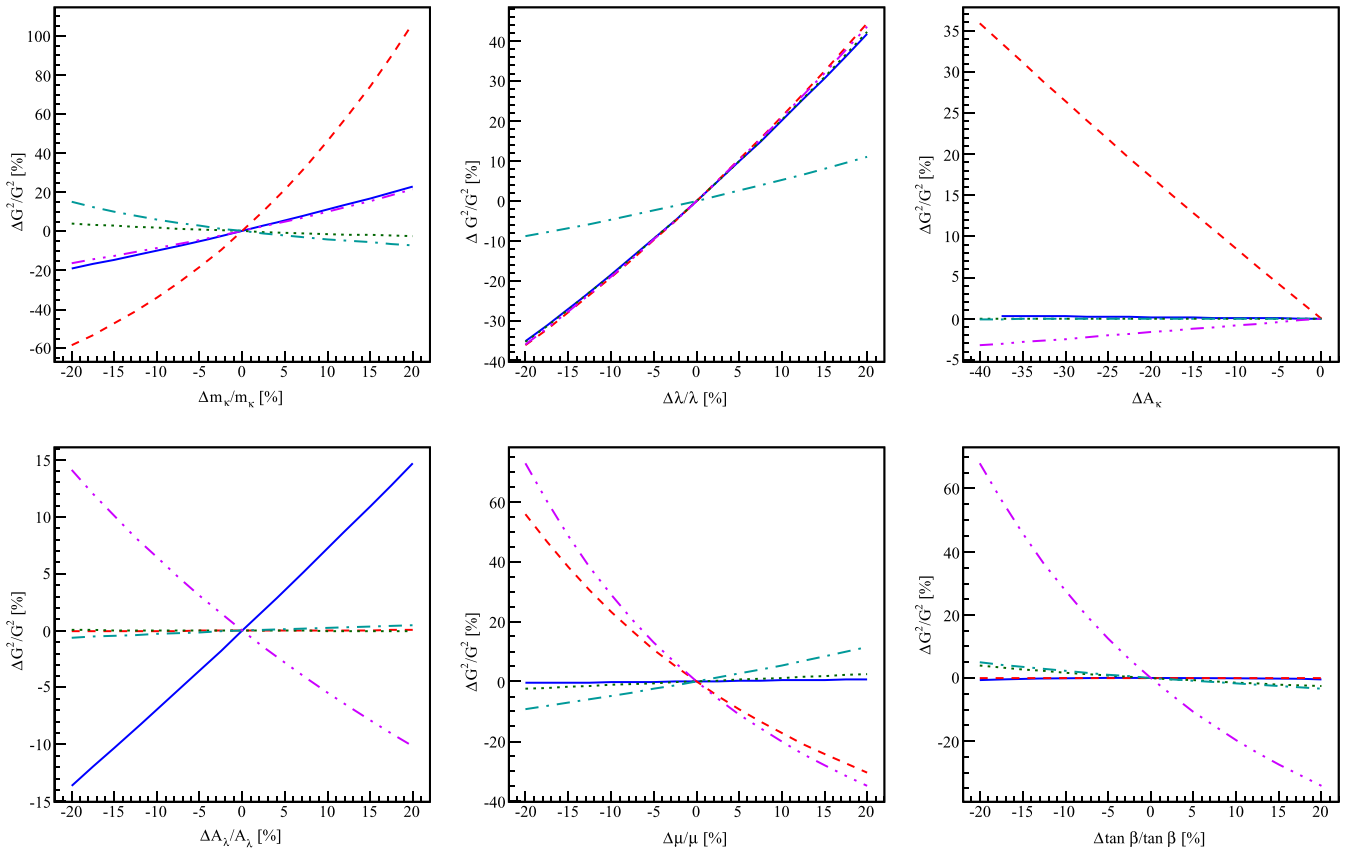

FIG. 1. Parameter dependence of (the square) of the couplings that enter some important decays, which we will study at one loop. We look at the variation in the parameters t_β, $\lambda, m_\kappa, A_\kappa, A_\lambda$, and μ. Plotted is the percentage variation measured from the reference point, defined in Table I. We allow variations of $\pm 20\%$ for these parameters apart from A_κ whose reference value, $A_\kappa = 0$, is varied smoothly up to 40 GeV. The solid (blue) lines represent the $h_3^0 h_2^0 h_1^0$ coupling, the dash-dot-dot-dotted (purple) lines the $A_2^0 Z^0 h_2^0$ coupling, the dotted (green) lines the $h_3^0 \tilde{\chi}_1^0 \tilde{\chi}_3^0$ coupling, the dashed (red) lines the $h_2^0 A_1^0 A_1^0$ coupling, the dash-dotted (turquoise) lines the $A_2^0 \to \tilde{\chi}_1^0 \tilde{\chi}_1^0$ coupling, and the long-dashed (gray) lines the $A_2^0 \tilde{\chi}_1^+ \tilde{\chi}_1^-$ coupling.

(iii) Decays involving both singlets and MSSM-like particles. $h_3^0 \to h_2^0 h_1^0, A_2^0 \to Z^0 h_2^0$ [and its $SU(2)$ equivalent $H^+ \to W^+ h_2^0$], and $h_3^0 \to \tilde{\chi}_1^0 \tilde{\chi}_3^0$. These decays are therefore sensitive to the mixing parameters due to the addition of the singlet in the NMSSM. For most decays this mixing parameter is essentially λ while for $h_3^0 h_2^0 h_1^0$ and $A_2^0 \to Z^0 h_2^0$, A_λ is also crucial.

We first look at the decays which involve only singlets and then none of them.

(i) $h_2^0 \to A_1^0 A_1^0$.

Similar to the self-coupling of the three CP-even neutral Higgs singlets in Eq. (2.35), with $A_\kappa = 0$ (at tree level), the $h_2^0 A_1^0 A_1^0$ interaction stems from the term $\kappa^2 S^4$ of the Higgs potential, Eq. (2.4). This trilinear coupling is controlled by $\kappa^2 s \propto m_\kappa^2/s \propto \lambda/\mu m_\kappa^2$. The relative variation of the square of the coupling

$$\frac{\Delta G^2_{h_2^0 A_1^0 A_1^0}}{G^2_{h_2^0 A_1^0 A_1^0}} \sim 2\left(\frac{\Delta\lambda}{\lambda} + 2\frac{\Delta m_\kappa}{m_\kappa} - \frac{\Delta\mu}{\mu}\right) \quad (8.2)$$

is well rendered by this simple observation and corresponds very well to the variations shown in Fig. 1. The small ΔA_κ variation in Fig. 1 can be explained similarly from the Higgs potential. Considering that this coupling is solely within the singlet sector, it is important to stress that the λ dependence here is due to our choice of m_κ (rather than κ), λ, μ as independent parameters.

(ii) $A_2^0 \to \tilde{\chi}_1^0 \tilde{\chi}_1^0$ and $A_2^0 \to \tilde{\chi}_1^+ \tilde{\chi}_1^-$.

$A_2^0 \to \tilde{\chi}_1^+ \tilde{\chi}_1^-$ is a MSSM-like decay with a very small dependence on the mixing λ scenario and practically independent of all other parameters. $h_3^0 \to \tilde{\chi}_1^+ \tilde{\chi}_1^-$ shares these same features. $A_2^0 \to \tilde{\chi}_1^0 \tilde{\chi}_1^0$ is quite similar, however, with some small dependence that creeps in from the mixing between the neutralinos. Still, as seen from Fig. 1 the λ dependence is 4 times smaller, $\Delta\lambda/2\lambda$, as compared to the situation when a singlet state is involved in the decay. One can also note a small dependence on μ (recall that the lightest neutralino is Higgsino-like) as well as some t_β dependence. Overall the parametric

dependence for the decay $A_2^0 \to \tilde{\chi}_1^0\tilde{\chi}_1^0$ can be approximated as

$$\frac{\Delta G^2_{A_2^0\tilde{\chi}_1^0\tilde{\chi}_1^0}}{G^2_{A_2^0\tilde{\chi}_1^0\tilde{\chi}_1^0}} \sim \frac{1}{2}\left(\frac{\Delta\lambda}{\lambda}+\frac{\Delta\mu}{\mu}-\frac{\Delta m_\kappa}{m_\kappa}-\frac{1}{2}\frac{\Delta t_\beta}{t_\beta}\right). \tag{8.3}$$

We now turn to the decays that involve a mixture of singlets/doublets states.

(i) $h_3^0 \to h_1^0 h_2^0$.

This decay is triggered from the coupling $h_u^0 h_d^0 h_s^0$ whose strength is controlled by $\lambda(A_\lambda + 2m_\kappa)$; see the term (3,1,2) in Eq. (2.35). With the values of m_κ and A_λ, this dependence gives a relative variation

$$\begin{aligned}\frac{\Delta G^2_{h_3^0 h_1^0 h_2^0}}{G^2_{h_3^0 h_1^0 h_2^0}} &\sim 2\left(\frac{\Delta\lambda}{\lambda}+\frac{A_\lambda}{A_\lambda+2m_\kappa}\frac{\Delta A_\lambda}{A_\lambda}\right.\\ &\quad\left.+\frac{2m_k}{A_\lambda+2m_\kappa}\frac{\Delta m_\kappa}{m_\kappa}\right)\\ &\sim 2\left(\frac{\Delta\lambda}{\lambda}+0.38\frac{\Delta A_\lambda}{A_\lambda}+0.6\frac{\Delta m_\kappa}{m_\kappa}\right),\end{aligned} \tag{8.4}$$

which is extremely well exhibited in Fig. 1.

(ii) $h_3^0 \to \tilde{\chi}_1^0\tilde{\chi}_3^0$.

This coupling is practically independent of the dimensionful parameters; it is not generated in the Higgs potential. The coupling is essentially dependent only on the mixing λ, with a very small t_β dependence, as confirmed by Fig. 1. The variation, for the square of the coupling, can be parametrized as

$$\frac{\Delta G^2_{h_3^0\tilde{\chi}_1^0\tilde{\chi}_3^0}}{G^2_{h_3^0\tilde{\chi}_1^0\tilde{\chi}_3^0}} \sim 2\frac{\Delta\lambda}{\lambda}. \tag{8.5}$$

(iii) $A_2^0 \to h_2^0 Z^0$.

The coupling responsible for this decay derives in part from $h_s^0 a_d^0 Z^0$, and therefore the singlet-doublet mixing is an essential ingredient. It is not a surprise that the λ dependence is the same as with all other decays in this class. As with the Higgs self-couplings, the A_λ mixing is not negligible as well as the t_β and μ dependences that enter through the mixing in the CP-odd and CP-even Higgs sectors. Apart from the λ dependence, deriving an analytical formula for the relative variation is difficult. Approximately we get

$$\begin{aligned}\frac{\Delta G^2_{ZA_2^0h_2^0}}{G^2_{ZA_2^0h_2^0}} &\sim 2\left(\frac{\Delta\lambda}{\lambda}-0.3\frac{\Delta A_\lambda}{A_\lambda}-\frac{\Delta t_\beta}{t_\beta}\right.\\ &\quad\left.+0.4\frac{\Delta m_\kappa}{m_\kappa}-1.2\frac{\Delta\mu}{\mu}\right).\end{aligned} \tag{8.6}$$

This is in good agreement with the behavior seen in Fig. 1. For later reference, observe also that it is this coupling and the $h_1^0 h_2^0 h_3^0$ that are most sensitive to a variation in A_λ, albeit with opposite trends.

2. Point A: Finite part of the counterterms and their β constant

The $\beta_{\mathbb{p}_i}$ constants that we extract numerically (see Sec. VI A) are given in units of 10^{-3},

$$\beta_\mu = 5.70, \tag{8.7}$$

$$\beta_{t_\beta} = 8.44, \tag{8.8}$$

$$\beta_\lambda = 5.83, \tag{8.9}$$

$$\beta_{m_\kappa} = 0.510, \tag{8.10}$$

$$\beta_{A_\lambda} = 548.74. \tag{8.11}$$

Since $A_\kappa = 0$, β_{A_κ} is not amenable to a numerical extraction. However, we have checked that δA_κ never plays a significant role, so we will omit it from our discussion. The most striking observation is that β_{A_λ} is very large; it is practically 2 orders of magnitude larger than the β of all the other parameters. In sharp contrast, note the tiny β_{m_κ}. When we recall that for this point the ratio A_t/A_λ is very large, $A_t/A_\lambda \sim 27$, these findings are not surprising [see Eqs. (6.8)]. We therefore expect a large scale dependence in the $\overline{\rm DR}$ scheme and probably a large correction for those branching ratios that are most sensitive to A_λ. A glance at Fig. 1 indicates that $h_3^0 \to h_1^0 h_2^0$ and $A_2^0 \to Z h_2^0$ [and its SU(2) equivalent $H^+ \to W^+ h_2^0$] are two such observables.

We have also derived the finite parts of the corresponding counterterms. For this benchmark we take $\bar{\mu} = Q_{\rm susy} = 1117.25$ GeV [see Eq. (8.1)]. As mentioned in Sec. VII, to ensure an *a priori* good extraction of the finite parts, we computed these finite parts in the schemes $t_{134A_1A_2}$ and $\mathrm{OS}_{34h_2A_1A_2H+}$. The results are given in Table IV.

We note that at the level of the counterterms, the scheme dependence in μ and m_κ is extremely small (less than 1%) and that in both schemes the values of these two counterterms are quite small. This is no surprise since μ can be extracted almost directly from one of the chargino masses while m_κ was chosen as an independent parameter precisely because it is an almost direct measure of the singlino mass in this small λ limit. As for the counterterms for A_λ, λ, and t_β we have large corrections. In the OS scheme $\delta A_\lambda/A_\lambda$ is more than 100% and $\delta t_\beta/t_\beta$ is also large. One would think that the use of M_{H^+} as an input in the OS scheme would have constrained $\delta A_\lambda/A_\lambda$ far better. In fact, as can be derived from the expression of the charged Higgs mass, Eq. (2.19), in the limit of small λ and rather large t_β, as is the case here, $\delta M^2_{H^+}/M^2_{H^+} \sim (\delta A_\lambda/A_\lambda + 1.8\delta t_\beta/t_\beta)/2$. Therefore it

TABLE IV. Finite parts of the various counterterms that play a role in the parametric dependence of the partial widths computed at $\bar{\mu} = Q_{\rm susy} = 1117.25$ GeV.

Scheme	$\delta\mu/\mu$	$\delta t_\beta/t_\beta$	$\delta\lambda/\lambda$	$\delta m_\kappa/m_\kappa$	$\delta A_\lambda/A_\lambda$
$t_{134A_1A_2}$	−2.42%	0	62.26%	−0.67%	−5.49%
$\overline{\rm OS}_{34h_2A_1A_2H+}$	−1.57%	−80.69%	−7.88%	0.3%	134%

is only the combination $(\delta A_\lambda/A_\lambda + 1.8\delta t_\beta/t_\beta)$ of these two counterterms that is well constrained. This is corroborated by the values of these two counterterms in Table IV. This issue with t_β is similar to the one encountered in the MSSM where the Higgs masses alone are not efficient to reconstruct t_β [45]. The good extraction of $\delta A_\lambda/A_\lambda$ in the $t_{134A_1A_2}$ scheme is therefore a result of the $\overline{\rm DR}$ condition $\delta t_\beta/t_\beta = 0$. This said, the $t_{134A_1A_2}$ scheme gives a bad reconstruction of $\delta\lambda/\lambda$. As argued in [44], in this small λ limit, the chargino/neutralino masses are not sensitive to λ. This leads to a large uncertainty on $\delta\lambda/\lambda$. The Higgs system with the inclusion of the singlet dominated h_2^0 in the OS scheme fares better as demonstrated in Table IV.

To summarize, we foresee (i) in the $\overline{\rm DR}$ scheme, a large scale variation for decays and couplings that feature a non-negligible dependence on A_λ ($h_3^0 \to h_1^0 h_2^0$, $A_2^0 \to Z h_2^0$, and $H^+ \to W^+ h_2^0$). The correction should minimize for $\bar{\mu} = Q_{\rm susy}$, (ii) in the $t_{134A_1A_2}$ scheme the corrections should be mainly driven by $\delta\lambda$. Since β_λ is small, the scale dependence in this mixed scheme is negligible. All decays are affected expect those not involving any singlet state, (iii) in the OS scheme one should pay special attention to those observables where the A_λ dependence is important and to a lesser extent the t_β dependence.

3. Full one-loop results

Full one-loop results for a variety of Higgs decays are shown in Table V. For each decay we give the result for the mixed $t_{134A_1A_2}$ scheme, the on-shell scheme $\overline{\rm OS}_{34h_2A_1A_2H^+}$, and the full $\overline{\rm DR}$ scheme. For the $t_{134A_1A_2}$ scheme we set the scale at $Q_{\rm susy} = 1117.25$ GeV. For the $\overline{\rm DR}$ scheme we consider an implementation both with a scale at $Q_{\rm susy}$ and with a scale Q_M that corresponds to the mass of the decaying Higgs. For the important decays of h_3^0, A_2^0, H^+, $Q_M \sim Q_{\rm susy}/2$. A quick glance at the table reveals that the corrections in the $\overline{\rm DR}$ scheme at $Q_{\rm susy}$ are quite small in practically all channels. The same results at the scale Q_M are within 2% *except* for the notable decays $h_3^0 \to h_1^0 h_2^0$, $A_2^0 \to Z h_2^0$, and $H^+ \to W^+ h_2^0$ as a consequence of the very large β_{A_λ}. The results in the mixed scheme show a very large and almost common correction of order 120%! (due to the large $\delta\lambda/\lambda \sim 62\%$ in this scheme) except for $h_3^0 \to \tilde{\chi}_1^+\tilde{\chi}_1^-$, $A_2^0 \to \tilde{\chi}_1^+\tilde{\chi}_1^-$, and $A_2^0 \to \tilde{\chi}_1^0\tilde{\chi}_1^0$. The corrections in the OS scheme are small to moderate *except* for the same notable decays where the scale dependence in the $\overline{\rm DR}$ scheme is large, $h_3^0 \to h_1^0 h_2^0$, $A_2^0 \to Z h_2^0$, and $H^+ \to W^+ h_2^0$. Following our discussion on the parametric dependence and the values of the counterterms, as well as the β functions, these results are easily understood. In fact, this is in perfect agreement with the arguments we summarized at the end of the preceding subsection.

The smallness of the radiative corrections in the $\overline{\rm DR}$ scheme seems to indicate that $\bar{\mu} \sim Q_{\rm susy}$ is the effective scale for all the decays in this model. This is also indicative that genuine corrections beyond the running of the parameters are quite small. We can be more quantitative about the differences between the schemes and the scale dependencies by combining the parametric dependencies derived from tree-level considerations in Eqs. (8.2)–(8.6) with the values of the finite parts of the counterterms in Table IV, which is $\Delta\mathbb{p}_i \to \delta\mathbb{p}_i$. Let us go through the results of some of the decays.

(i) $h_2^0 \to A_1^0 A_1^0$.

The scheme dependence of the relative correction to the decay is contained in $2(\delta\lambda/\lambda + 2\delta m_\kappa/m_\kappa - \delta\mu/\mu) \sim 2\delta\lambda/\lambda$. This contribution from the finite part of the counterterms gives practically the full one-loop correction in all the schemes; for instance, in the OS scheme this contribution returns a −11.4% correction by using the values given in Table IV. This is another manifestation that genuine corrections from three-point function contributions are negligible. The scale dependence for the $\overline{\rm DR}$ scheme is tiny, indeed with the negligible β_{m_κ} and with $\beta_\lambda \sim \beta_\mu$ the difference in the correction between the scale $Q_{\rm susy}$ and $m_{h_2^0}$ [using the general formula of Eq. (6.6) for the amplitude] is $2(\beta_\lambda + 2\beta_{m_\kappa} - \beta_\mu)\ln(m_{h_2^0}^2/Q_{\rm susy}^2) \sim -0.7\%$. This difference is an excellent approximation to the full one-loop result.

(ii) $A_2^0 \to \tilde{\chi}_1^0\tilde{\chi}_1^0$, $A_2^0 \to \tilde{\chi}_1^+\tilde{\chi}_1^-$, and $h_3^0 \to \tilde{\chi}_1^+\tilde{\chi}_1^-$.

We classified these decays in the second category where all particles involved in these decays are MSSM-like though with a very small singlet component for the neutralino case. We note that for these decays the scheme dependence is much smaller as compared to the other categories. In particular, these are the only decays where the relative one-loop corrections are under control in the $t_{134A_1A_2}$ scheme. The largest correction in this class shows up for $A_2^0 \to \tilde{\chi}_1^0\tilde{\chi}_1^0$ in the $t_{134A_1A_2}$ scheme driven essentially by the large value of $\delta\lambda$ despite the small parametric dependence of this parameter. Indeed, Eq. (8.3) when interpreted in terms of counterterms is an excellent explanation of the results we find for the full corrections and the scheme dependence.

(iii) $h_3^0 \to h_1^0 h_2^0$.

Apart from the $\overline{\rm DR}$ scheme with a scale at $Q_{\rm susy}$ where the correction is modest, all other schemes lead

TABLE V. Partial decay widths of Higgs bosons in other Higgs bosons and/or neutralinos, charginos, and gauge bosons at tree level (in MeV) and the percentage relative full one-loop correction, in the mixed scheme where only t_β is taken $\overline{\rm DR}$ ($t_{134A_1A_2}$), the evaluation is made at the scale $Q_{\rm susy}$, the full OS scheme and full $\overline{\rm DR}$ at two scales, Q_M is taken to be the mass of the decaying particle (see text for details of the schemes).

		One loop			
	Tree level [MeV]	$t_{134A_1A_2}$	$\mathrm{OS}_{34h_2A_1A_2H^+}$	$\overline{\rm DR}Q_M$	$\overline{\rm DR}Q_{\rm susy}$
$h_2^0\to A_1^0A_1^0$	47.9	128%	−12%	0.4%	−0.4%
$h_3^0\to h_1^0h_2^0$	22.1	116%	79%	52%	−1.7%
$h_3^0\to\tilde\chi_1^0\tilde\chi_3^0$	35.2	122%	−3%	2%	0.3%
$h_3^0\to\tilde\chi_2^0\tilde\chi_3^0$	33.8	126%	−35%	3%	1.1%
$h_3^0\to\tilde\chi_1^+\tilde\chi_1^-$	45.5	1%	−11%	−9%	−7.4%
$A_2^0\to Z^0h_2^0$	18.6	120%	80%	−56%	−14.5%
$A_2^0\to\tilde\chi_1^0\tilde\chi_1^0$	33.0	28%	13%	0.3%	−1.6%
$A_2^0\to\tilde\chi_1^0\tilde\chi_3^0$	24.4	130%	−31%	8%	6.2%
$A_2^0\to\tilde\chi_2^0\tilde\chi_3^0$	30.2	122%	−5%	−0.4%	−1.9%
$A_2^0\to\tilde\chi_1^+\tilde\chi_1^-$	55.1	−10%	−1.5%	−6%	−8%
$H^+\to W^+h_2^0$	20.1	119%	79%	−56%	−16%
$H^+\to\tilde\chi_1^+\tilde\chi_3^0$	64.0	125%	−18%	3%	1.1%

to large corrections. We verify, based on the parametric dependence in Eq. (8.4) and on the fact that $\beta_{A_\lambda}\gg\beta_\lambda\gg\beta_{m_\kappa}$, that the difference between the scales in $\overline{\rm DR}$ is indeed given by $2\times0.38\beta_{A_\lambda}\ln(m^2_{h_3^0}/Q^2_{\rm susy})\sim-54\%$. The values for the corrections in the OS scheme and the mixed scheme are also very well approximated by the parametric dependence upon replacing the variations by the corresponding counterterms found in Table IV. In the OS scheme the correction is driven essentially by the poor extraction of A_λ while in the mixed scheme it is again essentially the imprecise input $\delta\lambda/\lambda$ that is behind the large correction.

(iv) $A_2^0\to Z^0h_2^0$ and the equivalent $H^+\to W^-h_2^0$.

Because of the large running A_λ, it is sufficient to consider A_λ when comparing the results in the $\overline{\rm DR}$ scheme at the two scales. The parametric dependence, Eq. (8.6), explains very well the ∼40% difference between the two scales in the $\overline{\rm DR}$ scheme. The difference between the OS scheme and the $\overline{\rm DR}$ at $Q_{\rm susy}$ is driven essentially by the determination of A_λ and t_β, both of which are badly derived in the OS scheme, whereas the discrepancy in the mixed scheme comes once again from a bad reconstruction of λ.

(v) All the remaining decays of Table IV are those where the Higgses (*CP*-even, *CP*-odd, or charged) are decaying into neutralinos/charginos involving the mostly singlet $\tilde\chi_3^0$. These decays would vanish in the $\lambda\to0$ limit. We studied the parametric dependence of a representative of these decays earlier, $h_3^0\to\tilde\chi_1^0\tilde\chi_3^0$. We verified the strong λ dependence, and noted a small t_β dependence (which takes place in the neutralino/chargino sector). Translated in terms of counterterms, the parametric dependence is $2\delta\lambda/\lambda$, which again explains extremely well the almost uniform large correction, ∼120%, in the $t_{134A_1A_2}$ scheme. In the OS scheme, the corrections are much smaller but the residual t_β dependence in some of these decays is not totally negligible.

Point A is somehow pathological in the sense that it is MSSM-like and the amount of mixing is small. This makes it difficult to reconstruct all the parameters rather precisely. The OS scheme would perform well if it were not penalized by a very imprecise reconstruction of t_β, which impacts badly on the reconstruction of A_λ. The mass of the charged Higgs as an input only constrains a very specific combination of these two parameters. The MSSM is fraught with the same problem of a reconstruction of t_β from the Higgs masses alone. We have shown that in the MSSM a very good scheme for extracting t_β relied on the decay $A^0\to\tau^-\tau^-$ [45]. In the NMSSM, this issue needs to be investigated in depth and is left for a future work.

B. Point B

The most crucial features to keep in mind when reviewing the results for Point B, especially after what we have seen for Point A, is the fact that λ is large (and t_β small) and A_λ is smaller than A_t by only a factor of 2. The last observation should mean that β_{A_λ} should not be excessively large. With such a value of λ (and A_λ) this point constitutes a genuine example of the NMSSM, and the branching ratios for the decays we consider here are at least an order of magnitude larger than in Point A. The difficulty now is that the notion of an almost singlet (and MSSM-like) state will be lost, couplings between the physical states will depend strongly on the pattern of the mixing matrices. The study of the parametric dependence of the couplings, and hence the decays, on the underlying parameters is here even more important. This is what we look at, at tree level, for a few decays for which we have calculated the full one-loop corrections.

1. Tree-level. Parameter dependence on some couplings

Figure 2 shows the variations of some couplings when some of the underlying parameters are perturbed within ±20%. For Point B we have also examined variations in M_1 and M_2, which we do not show in Fig. 2 to avoid clutter. The most striking difference with Point A is the fact that for the trilinear Higgs couplings, $h_3^0h_1^0h_2^0$, $h_3^0h_2^0h_2^0$, and $h_1^0A_1^0A_2^0$, the dependence on almost all parameters is large and highly

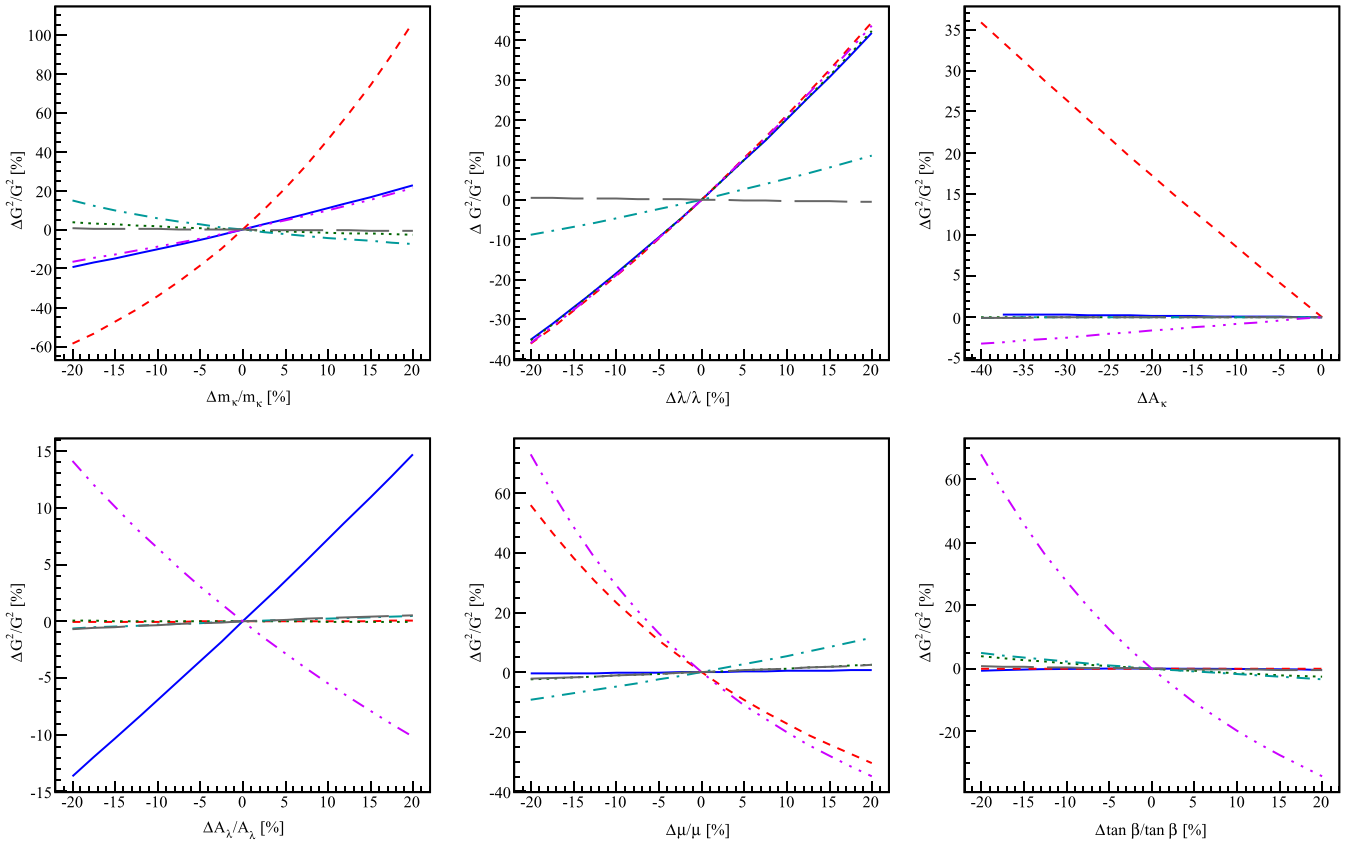

FIG. 2. Parameter dependence on (the square) of the couplings that enter some important decays that we will study at one loop. We look at the variation in the parameters t_β, $\lambda, m_\kappa, A_\kappa, A_\lambda$, and μ. Plotted is the percentage variation measured from the reference point. We allow variations of $\pm 20\%$ for these parameters apart from A_κ whose reference value, $A_\kappa = 0$, is varied smoothly up to 40 GeV. The solid (blue) lines represent the $h_3^0 h_2^0 h_1^0$ coupling, the long dash-dotted (purple) lines the $H^+ W^- A_1^0$ coupling, the dotted (green) lines the $A_2^0 A_1^0 h_1^0$ coupling, the dashed (red) lines the $h_3^0 h_2^0 h_2^0$ coupling, and the dash-dotted (turquoise) lines the $A_2^0 \tilde{\chi}_1^+ \tilde{\chi}_1^-$ coupling.

nonlinear even for parametric variations of about 10%. For example, a 10% change in A_λ around its reference value gives a variation of almost 100% on the trilinear Higgs couplings. Recall here that t_β is small, but we can see that small changes in this parameter give rise to dramatic changes in the trilinear coupling. Decays involving two Higgses and a gauge boson, one such coupling is $A_1^0 H^+ W^-$, show also large deviations though not as dramatic as for couplings involving three Higgses. Decays of the Higgs into neutralinos/charginos such as $A_2^0 \to \chi_1^+ \chi_1^-$ show much more moderate variations with practically an almost linear dependence. Although not shown in these figures, for decays into charginos and neutralinos the effect of a change in the gaugino masses M_1, M_2 is not totally negligible. For most decays the parameters that lead to the largest changes are A_λ, λ, μ, and t_β. Considering the highly nonlinear behavior of these variations, a linear parametrization is justified only for small variations. We will therefore first check whether the finite parts of the counterterms in this model are small enough. If so, we will give the parametrization as befits a one-loop correction where the counterterms enter only at first order.

In view of these preliminary observations, the two-body decays studied here can be classified into three categories depending on how many Higgses are taking part in the decay:

(i) a single Higgs for decays into neutralinos and charginos, the amplitude will then involve the matrix S_h.
(ii) two Higgses and a gauge boson where in this case the Higgses are of opposite parity hence involving the product of the diagonalizing matrices $S_h \times P_a$.
(iii) three Higgses where in the case of three neutral CP-even Higgs the elements of $(S_h)^3$ enter and in the case of a CP-even Higgs decaying into two pseudoscalars the amplitudes call for $S_h \times P_a^2$.

The dependence of these mixing matrices on the underlying parameters, in particular λ, A_λ, is highly nonlinear when λ is not small. In the latter case one expects that when more and more Higgses are involved, as, for instance, in the case of the Higgs self-couplings, the mixing matrices introduce highly nontrivial dependencies.

TABLE VI. Finite parts of the various counterterms that play a role in the parametric dependence of the partial widths computed at $\bar{\mu} = Q_{\rm susy} = 753.55$ GeV.

Scheme	$\delta\mu/\mu$	$\delta t_\beta/t_\beta$	$\delta\lambda/\lambda$	$\delta m_\kappa/m_\kappa$	$\delta A_\lambda/A_\lambda$
$t_{123A_1A_2}$	−1.04%	0	3.71%	−1.5%	6.85%
$\mathrm{OS}_{12h_2A_1A_2H^+}$	−1.63%	6.50%	5.94	−1.52%	3.40%

2. Point B: Finite part of the counterterms and their β constant

We first list the β functions; in units of 10^{-3} they are

$$\beta_\mu = 7.13, \tag{8.12}$$

$$\beta_{t_\beta} = -8.81, \tag{8.13}$$

$$\beta_\lambda = 10.22, \tag{8.14}$$

$$\beta_{m_\kappa} = 6.19, \tag{8.15}$$

$$\beta_{A_\lambda} = 61.36. \tag{8.16}$$

As expected, since the ratio A_t/A_λ has decreased by about a factor of 10 compared to Model A, the value of β_{A_λ} has decreased by almost an order of magnitude; see Eq. (6.8). Yet, this is still the largest β constant (6% rather than 1% for the others).

The finite part of the counterterms (evaluated at $Q_{\rm susy} \sim 754$ GeV) that we extract are given in Table VI. All counterterms are of the same order, none exceeding 7%, and in any case they are much smaller than some of the large values we found for Point A. This rather precise extraction has to do with the fact that, because of the not so small mixing, a large number of observables, in particular masses, are quite sensitive to the underlying parameters. The fact that these values are not very large justifies parametrizing the variation at first order in the counterterm. The first derivative of the variation, at the origin, gives the infinitesimal parametrization.

3. One-loop results and analysis of scheme dependence

A quick inspection of the results in Table VII reveals that, if we leave out the decays of the category involving the trilinear Higgs couplings, in particular the *CP*-even $h_3^0 \to h_1^0 h_2^0, h_2^0 h_2^0$, the radiative corrections are moderate, especially compared to Point A. Overall, the OS scheme performs quite well. In particular, the OS scheme returns the smallest corrections for the problematic decays $h_3^0 \to h_1^0 h_2^0, h_2^0 h_2^0$. Still, in most cases the scheme dependence is not negligible. This is not surprising considering the abrupt variations we observed at tree level on the Higgs trilinear couplings.

TABLE VII. Partial decay widths of Higgs bosons in other Higgs bosons and/or neutralinos, charginos, and gauge bosons at tree level (in GeV) and the percentage relative full one-loop correction, in the mixed scheme where only t_β is taken $\overline{\rm DR}$ ($t_{134A_1A_2}$) at the scale $Q_{\rm susy}$, the full OS scheme, and the full $\overline{\rm DR}$ schemes at two scales. Q_M is taken to be the mass of the decaying particle.

		One loop			
	Tree level [GeV]	$t_{123A_1A_2}$	$\mathrm{OS}_{12h_2A_1A_2H^+}$	$\overline{\rm DR}Q_M$	$\overline{\rm DR}Q_{\rm susy}$
$h_3^0 \to \tilde{\chi}_1^0\tilde{\chi}_2^0$	0.726	13.3%	14%	5%	3%
$h_3^0 \to A_1^0 Z^0$	0.613	13%	3%	−3%	8%
$h_3^0 \to h_2^0 h_1^0$	0.341	−142%	−25%	−106%	−50%
$h_3^0 \to h_2^0 h_2^0$	0.514	51%	6%	13%	−28%
$A_2^0 \to \tilde{\chi}_1^+\tilde{\chi}_1^-$	1.523	9%	7%	2%	1%
$A_2^0 \to \tilde{\chi}_1^0\tilde{\chi}_1^0$	0.723	19%	32%	2%	2%
$A_2^0 \to Z^0 h_2^0$	0.638	−10%	12%	−16%	−9%
$A_2^0 \to A_1^0 h_1^0$	0.415	−43%	−0.3%	−32%	−17%
$H^+ \to \tilde{\chi}_1^+\tilde{\chi}_2^0$	1.056	10%	6%	10%	8%
$H^+ \to W^+ h_2^0$	0.609	−11%	11%	−18%	−10%
$H^+ \to W^+ A_1^0$	0.603	12%	2%	−3%	−9%
$H^+ \to \tilde{\chi}_1^+\tilde{\chi}_1^0$	0.561	14%	21%	9%	9%

(i) Decays into charginos and neutralinos ($A_2^0 \to \tilde{\chi}_1^+\tilde{\chi}_1^-$, $A_2^0 \to \tilde{\chi}_1^0\tilde{\chi}_1^0$).

First observe that the scale dependence in these decays is never larger than 2%. This is due in a large part to the fact that the couplings involved in these decays are insensitive to A_λ, a parameter that comes with the largest β. The β constants for the other parameters are all smaller than 1%. Besides, as Fig. 2 confirms for $A_2^0 \to \tilde{\chi}_1^+\tilde{\chi}_1^-$, the parametric dependence is quite small for these decays compared to those where more than one Higgs is involved. We can write

$$\frac{\delta\Gamma_{A_2^0\to\tilde{\chi}_1^+\tilde{\chi}_1^-}}{\Gamma^0_{A_2^0\to\chi_1^+\chi_1^-}} \sim 0.67\frac{\delta\lambda}{\lambda} + 0.55\frac{\delta\mu}{\mu} - 0.3\frac{\delta t_\beta}{t_\beta}. \tag{8.17}$$

The differences between schemes are within about 10%, and the smallest corrections are usually obtained in the $\overline{\rm DR}$ scheme. The scheme dependence is quite small for all the decays in this category apart from the special case of $A_2^0 \to \tilde{\chi}_1^0\tilde{\chi}_1^0$. $\tilde{\chi}_1^0$ here is dominated by the bino component but with a large wino and Higgsino component. In this case we have worked out the parametric dependence including the M_1 and M_2 counterterms,

$$\frac{\delta\Gamma_{A_2^0\to\tilde{\chi}_1^0\tilde{\chi}_1^0}}{\Gamma^0_{A_2^0\to\tilde{\chi}_1^0\tilde{\chi}_1^0}} \sim 1.1\frac{\delta\lambda}{\lambda} - 2.4\frac{\delta\mu}{\mu} + 0.9\frac{\delta t_\beta}{t_\beta} + 2.6\frac{\delta M_1}{M_1} - 0.9\frac{\delta M_2}{M_2} - 0.9\frac{\delta m_\kappa}{m_\kappa}. \quad (8.18)$$

The ∼10% difference between the $t_{123A_1A_2}$ and the OS scheme is essentially due to the t_β definition in the two schemes. The relatively large correction of 32% in the OS scheme is, in fact, due to the addition of many smaller contributions including M_1, M_2 (and μ), which all affect the neutralino sector.

(ii) Higgs decays into a vector boson and another Higgs ($A_2 \to Z^0 h_2^0, H^+ \to W^+ h_2^0, H^+ \to W^+ A_1^0, h_3^0 \to A_1^0 Z^0$).

The pattern of the corrections for these decays is quite similar. In all the schemes, the one-loop corrections are moderate. They are, in absolute terms, within 20% with a scheme difference that can attain 30%. In $\overline{\rm DR}$ the scale dependence is about 6% when we compare the values obtained at $Q_{\rm susy} \sim 754$ GeV and at a scale about the mass of the decaying Higgs ∼480 GeV. For $H^+ \to W^+ A_1^0$, this is accounted for by the A_λ running $\kappa^{HWA}_{A_\lambda}\beta_{A_\lambda}\ln(Q^2_{\rm SUSY}/M^2_{H^\pm})$ with $\kappa^{HWA}_{A_\lambda} \sim 1$ as can be inferred from Fig. 2.

(iii) $h_3^0 \to h_2^0 h_1^0$.

With three Higgses involved in the process, the parametric dependence becomes very important. Because of the large value of β_{A_λ} compared to all other β's, one still expects the running to be dominated by this parameter. Indeed, the corrections in the $\overline{\rm DR}$ schemes are not only quite large, −50% at $Q_{\rm susy} \sim 754$ GeV, but they are also very sensitive to the choice of scale since at the scale M_{H^+}, which is not even half $Q_{\rm susy}$, the corrections more than double to −106%. This is driven by the large variation due to A_λ as observed in Fig. 2. One can approximate the variation as $10\beta_{A_\lambda}\ln(Q^2_{\rm SUSY}/M^2_{h_3^0}) \sim 60\%$. In fact, the dependence in the counterterms can be worked out more precisely,

$$\frac{\delta\Gamma_{h_3^0h_2^0h_1^0}}{\Gamma^0_{h_3^0h_2^0h_1^0}} \sim 1.3\frac{\delta\lambda}{\lambda} + 16\frac{\delta\mu}{\mu} + 11\left(1.15\frac{\delta t_\beta}{t_\beta} - \frac{\delta A_\lambda}{A_\lambda}\right) + 0.2\frac{\delta m_\kappa}{m_\kappa}. \quad (8.19)$$

With the extracted values of the counterterms in the OS and mixed schemes (written for $\bar{\mu} = Q_{\rm susy}$) we recover the differences shown in Table VII between the OS and $\overline{\rm DR}$ and t schemes. Note also the "compensation" between the variation in t_β and A_λ in the parametric dependence, which is effective in keeping the correction in the OS scheme manageable.

Although the scheme dependence is well understood, the fact that the corrections in the $\overline{\rm DR}$ scheme at the scale $Q_{\rm susy}$ are large indicates that this scale is not the most appropriate effective scale that minimizes the correction. In this respect the OS scheme gives a more "perturbative" prediction. Nonetheless, a scale of $Q_{\rm eff} \sim 1.5 Q_{\rm susy}$ gives a correction of only about 1%. An effective scale $\sim 1.2 Q_{\rm susy}$ reproduces the result of the OS scheme. This shows that small changes in the scale (around $Q_{\rm susy}$) reduce the results quite significantly. This is driven mostly by the large sensitivity in some of the parameters, essentially A_λ whose β constant is the largest.

(iv) $h_3^0 \to h_2^0 h_2^0$.

The parametric dependence that tracks the dominant variations are also very large here as we remarked earlier. It can be approximated as

$$\frac{\delta\Gamma_{h_3^0h_2^0h_2^0}}{\Gamma^0_{h_3^0h_2^0h_2^0}} \sim 4\frac{\delta\lambda}{\lambda} - 8\left(\frac{\delta\mu}{\mu} + \frac{1}{2}\frac{\delta t_\beta}{t_\beta} - \frac{\delta A_\lambda}{A_\lambda}\right) + 0.3\frac{\delta m_\kappa}{m_\kappa}. \quad (8.20)$$

We note that although the A_λ dependence is large, it is not as large as the one found for the $h_1^0 h_2^0 h_3^0$ coupling. Indeed, before performing the diagonalization to the physical basis, this coupling would stem from the $h_s^0 h_s^0 h_d^0$ part of the potential whose strength is $\lambda^2 v_d \propto \lambda^2 c_\beta$. This also explains the quartic dependence on λ of the coupling. Even though the parametric dependence on A_λ is more moderate than for $h_3^0 h_2^0 h_1^0$, it remains a strong parametric dependence in this decay also. Add to this the fact that β_{A_λ} is the largest of all β, the large scale dependence is driven essentially by β_{A_λ}. For the coupling responsible for this decay, an effective scale about twice lower than what was found in $h_3^0 h_2^0 h_1^0$ is required to bring the corrections to a negligible level. Varying again by $30\% Q_{\rm susy}$ brings the $\overline{\rm DR}$ corrections in par with the correction in the OS scheme. Equation (8.20) when combined with the values of the finite part of the counterterms in the OS scheme given in Table VI reproduce very well the difference between the OS scheme and the $\overline{\rm DR}$ scheme.

(v) $A_2^0 \to A_1^0 h_1^0$.

For this decay the parametric dependence can be approximated by

$$\frac{\delta\Gamma_{A_2^0\to A_1^0h_1^0}}{\Gamma_{A_2^0\to A_1^0h_1^0}} \sim 0.9\frac{\delta\lambda}{\lambda} + 8.4\left(\frac{\delta\mu}{\mu} + \frac{9}{16}\frac{\delta t_\beta}{t_\beta} - \frac{7}{16}\frac{\delta A_\lambda}{A_\lambda}\right) - 1.1\frac{\delta m_\kappa}{m_\kappa}. \quad (8.21)$$

Once again, the correction for this trilinear Higgs coupling is smallest in the OS scheme. The scale dependence that can be seen from the two values in

the $\overline{\text{DR}}$ scheme is not small. As has been a pattern for other trilinear Higgs couplings, the rather large scale dependence is also a sign of a large correction in the mixed $t_{123A_1A_2}$ scheme. The scale dependence is driven essentially by β_{A_λ}. $Q_{\text{eff}} \sim 1.5 Q_{\text{susy}}$ is the effective scale where the corrections vanish in the $\overline{\text{DR}}$ scheme. Note that this is the same effective scale we found for $h_3^0 \to h_1^0 h_1^0$. The small correction in the OS scheme is a result of a cancellation between the contribution of the A_λ and t_β counterterms. Because in the t scheme, t_β is defined in $\overline{\text{DR}}$, this cancellation is not operative and again the correction is dominated by A_λ.

To summarize the results for Model B, it is worth stressing that in decays of Higgs into Higgses the OS scheme performs quite well in the sense that it gives very small corrections. There is a large scale dependence for these decays, but the effective scale where the correction vanishes in $\overline{\text{DR}}$ is, after all, not that much different from Q_{susy}. Although β_{A_λ} is about 6%, a value 10 times smaller than in Model A, the parametric dependence in Model B is strong, thus enhancing the loop correction. Decays into charginos and neutralinos being much less sensitive to A_λ do not show much scheme and scale dependence.

IX. CONCLUSIONS

With the renormalization of the Higgs sector, it is now possible to compute full one-loop electroweak and QCD corrections to masses, decays, and scattering processes in the NMSSM with SloopS. This is particularly relevant as experiments are improving the precision in the measurements of Higgs and dark matter observables. Our computation of partial decay widths illustrates the importance of pure electroweak corrections for Higgs decays into supersymmetric particles and highlights the choice of the renormalization scheme. Our setup allows us to choose between the $\overline{\text{DR}}$ scheme, different on-shell schemes, and "mixed" schemes whereby some conditions are imposed on on-shell quantities and others taken as $\overline{\text{DR}}$. This variety of schemes has been implemented within SloopS. Comparing different renormalization schemes is crucial to weigh the theoretical uncertainties and the possible necessity of higher order corrections. For this purpose, we discussed at length how the choice of the minimal set of physical masses to reconstruct the underlying parameters can affect the numerical results and their reliability. We have found large radiative corrections for some observables. Some of these large corrections appear only in certain renormalization schemes. In this case, when the scheme dependence is large, this can also be accompanied by a large scale dependence in the $\overline{\text{DR}}$ scheme. These large scheme dependencies and large scale variations are due to a large value of some β constants for some specific underlying parameters and/or are associated with a large parametric dependence of the observable upon this specific parameter. The latter situation occurs in a NMSSM with a moderate λ. In the small λ scenarios, this parametric dependence is not as large; however, many counterterms are poorly reconstructed precisely because they are extracted from a set of input masses with little sensitivity on some of the underlying parameters. It has to be stressed that, although easier to implement, taking only masses as inputs may not be the optimal choice to renormalize the model. When new particles are discovered, not only their masses will be measured but so will the strength of their production modes and their decays. These observables will thus offer new possibilities for reconstructing the fundamental parameters of the model that will not require the knowledge of the complete particle spectrum. It remains to be seen whether a more cleverly chosen renormalization scheme, for example, one that uses the partial width of a heavy Higgs decay as a renormalization condition, would lead to better controlled corrections. In the MSSM we have shown [45] that the decay of the pseudoscalar Higgs to a pair of τ's is an excellent definition of t_β. Some of the large corrections we found are also pathological in the sense that they are due to a rather large value of A_t compared to the NMSSM parameter A_λ. Such a discrepancy between A_t and A_λ is responsible for a large β_{A_λ}, which will then propagate into the corrections of many Higgs observables, in particular those for the Higgs self-couplings. A natural NMSSM should not require very large values of A_t as what is required for MSSM-like models (with $\lambda \ll 1$); in this case the one-loop corrections are contained and an on-shell scheme is a quite judicious choice.

ACKNOWLEDGMENTS

This research was supported in part by the Research Executive Agency (REA) of the European Union under the Grant Agreement No. PITN-GA2012-316704 ("HiggsTools"), by "Investissements d'avenir, Labex ENIGMASS," and by the French ANR, Project DMAstro-LHC, ANR-12-BS05-006. G. C. is supported in part by the ERC advanced grant Higgs@LHC and the THEORY-LHC France initiative of CNRS/IN2P3. The authors would like to thank A. Djouadi for useful discussions regarding the project.

[1] G. Aad *et al.* (ATLAS Collaboration), Observation of a new particle in the search for the Standard Model Higgs boson with the ATLAS detector at the LHC, Phys. Lett. B **716**, 1 (2012).
[2] S. Chatrchyan *et al.* (CMS Collaboration), Observation of a new boson at a mass of 125 GeV with the CMS experiment at the LHC, Phys. Lett. B **716**, 30 (2012).
[3] L. J. Hall, D. Pinner, and J. T. Ruderman, A natural SUSY Higgs near 126 GeV, J. High Energy Phys. 04 (2012) 131.
[4] U. Ellwanger, C. Hugonie, and A. M. Teixeira, The next-to-minimal supersymmetric Standard Model, Phys. Rep. **496**, 1 (2010).
[5] U. Ellwanger and C. Hugonie, The upper bound on the lightest Higgs mass in the NMSSM revisited, Mod. Phys. Lett. A **22**, 1581 (2007).
[6] U. Ellwanger, G. Espitalier-Noel, and C. Hugonie, Naturalness and fine tuning in the NMSSM: Implications of early LHC results, J. High Energy Phys. 09 (2011) 105.
[7] M. Bastero-Gil, C. Hugonie, S. F. King, D. P. Roy, and S. Vempati, Does LEP prefer the NMSSM?, Phys. Lett. B **489**, 359 (2000).
[8] G. G. Ross, K. Schmidt-Hoberg, and F. Staub, The generalised NMSSM at one loop: Fine tuning and phenomenology, J. High Energy Phys. 08 (2012) 074.
[9] S. Dittmaier *et al.* (LHC Higgs Cross Section Working Group Collaboration), Handbook of LHC Higgs cross sections: 1. Inclusive observables, arXiv:1101.0593.
[10] S. Dittmaier *et al.*, Handbook of LHC Higgs cross sections: 2. Differential distributions, arXiv:1201.3084.
[11] J. R. Andersen *et al.* (LHC Higgs Cross Section Working Group Collaboration), Handbook of LHC Higgs cross sections: 3. Higgs properties, arXiv:1307.1347.
[12] D. de Florian *et al.* (LHC Higgs Cross Section Working Group Collaboration), Handbook of LHC Higgs cross sections: 4. Deciphering the nature of the Higgs sector, arXiv:1610.07922.
[13] H. E. Haber and R. Hempfling, Can the Mass of the Lightest Higgs Boson of the Minimal Supersymmetric Model Be Larger than $m(Z)$?, Phys. Rev. Lett. **66**, 1815 (1991).
[14] J. R. Ellis, G. Ridolfi, and F. Zwirner, Radiative corrections to the masses of supersymmetric Higgs bosons, Phys. Lett. B **257**, 83 (1991).
[15] A. Djouadi, The anatomy of electro-weak symmetry breaking. II. The Higgs bosons in the minimal supersymmetric model, Phys. Rep. **459**, 1 (2008).
[16] M. Carena and H. E. Haber, Higgs boson theory and phenomenology, Prog. Part. Nucl. Phys. **50**, 63 (2003).
[17] S. P. Martin, Strong and Yukawa two-loop contributions to Higgs scalar boson self-energies and pole masses in supersymmetry, Phys. Rev. D **71**, 016012 (2005).
[18] S. Heinemeyer, MSSM Higgs physics at higher orders, Int. J. Mod. Phys. A **21**, 2659 (2006).
[19] U. Ellwanger, Radiative corrections to the neutral Higgs spectrum in supersymmetry with a gauge singlet, Phys. Lett. B **303**, 271 (1993).
[20] T. Elliott, S. F. King, and P. L. White, Squark contributions to Higgs boson masses in the next-to-minimal supersymmetric standard model, Phys. Lett. B **314**, 56 (1993).
[21] T. Elliott, S. F. King, and P. L. White, Radiative corrections to Higgs boson masses in the next-to-minimal supersymmetric Standard Model, Phys. Rev. D **49**, 2435 (1994).
[22] P. N. Pandita, One loop radiative corrections to the lightest Higgs scalar mass in nonminimal supersymmetric Standard Model, Phys. Lett. B **318**, 338 (1993).
[23] P. N. Pandita, Radiative corrections to the scalar Higgs masses in a nonminimal supersymmetric Standard Model, Z. Phys. C **59**, 575 (1993).
[24] U. Ellwanger and C. Hugonie, Yukawa induced radiative corrections to the lightest Higgs boson mass in the NMSSM, Phys. Lett. B **623**, 93 (2005).
[25] K. Ender, T. Graf, M. Muhlleitner, and H. Rzehak, Analysis of the NMSSM Higgs boson masses at one-loop level, Phys. Rev. D **85**, 075024 (2012).
[26] G. Degrassi and P. Slavich, On the radiative corrections to the neutral Higgs boson masses in the NMSSM, Nucl. Phys. **B825**, 119 (2010).
[27] M. D. Goodsell, K. Nickel, and F. Staub, Two-loop corrections to the Higgs masses in the NMSSM, Phys. Rev. D **91**, 035021 (2015).
[28] F. Staub, P. Athron, U. Ellwanger, R. Grober, M. Muhlleitner, P. Slavich, and A. Voigt, Higgs mass predictions of public NMSSM spectrum generators, Comput. Phys. Commun. **202**, 113 (2016).
[29] P. Drechsel, L. Galeta, S. Heinemeyer, and G. Weiglein, Precise predictions for the Higgs-boson masses in the NMSSM, Eur. Phys. J. C **77**, 42 (2017).
[30] P. Drechsel, R. Groeber, S. Heinemeyer, M. M. Muhlleitner, H. Rzehak, and G. Weiglein, Higgs-boson masses and mixing matrices in the NMSSM: Analysis of on-shell calculations, Eur. Phys. J. C **77**, 366 (2017).
[31] S. Liebler, Neutral Higgs production at proton colliders in the *CP*-conserving NMSSM, Eur. Phys. J. C **75**, 210 (2015).
[32] J. Baglio, T. N. Dao, R. Gröber, M. M. Mühlleitner, H. Rzehak, M. Spira, J. Streicher, and K. Walz, A new implementation of the NMSSM Higgs boson decays, EPJ Web Conf. **49**, 12001 (2013).
[33] J. Baglio, C. O. Krauss, M. Mühlleitner, and K. Walz, Next-to-leading order NMSSM decays with *CP*-odd Higgs bosons and stops, J. High Energy Phys. 10 (2015) 024.
[34] D. T. Nhung, M. Muhlleitner, J. Streicher, and K. Walz, Higher order corrections to the trilinear Higgs self-couplings in the real NMSSM, J. High Energy Phys. 11 (2013) 181.
[35] J. Baglio, R. Gröber, M. Mühlleitner, D. T. Nhung, H. Rzehak, M. Spira, J. Streicher, and K. Walz, NMSSMCALC: A program package for the calculation of loop-corrected Higgs boson masses and decay widths in the (complex) NMSSM, Comput. Phys. Commun. **185**, 3372 (2014).
[36] U. Ellwanger and C. Hugonie, NMHDECAY 2.0: An updated program for sparticle masses, Higgs masses, couplings and decay widths in the NMSSM, Comput. Phys. Commun. **175**, 290 (2006).
[37] U. Ellwanger and C. Hugonie, NMSPEC: A Fortran code for the sparticle and Higgs masses in the NMSSM with GUT scale boundary conditions, Comput. Phys. Commun. **177**, 399 (2007).
[38] F. Staub, W. Porod, and B. Herrmann, The electroweak sector of the NMSSM at the one-loop level, J. High Energy Phys. 10 (2010) 040.

[39] W. Porod and F. Staub, SPheno 3.1: Extensions including flavour, *CP*-phases and models beyond the MSSM, Comput. Phys. Commun. **183**, 2458 (2012).
[40] D. Das, U. Ellwanger, and A. M. Teixeira, NMSDECAY: A Fortran code for supersymmetric particle decays in the next-to-minimal supersymmetric Standard Model, Comput. Phys. Commun. **183**, 774 (2012).
[41] B. C. Allanach, P. Athron, L. C. Tunstall, A. Voigt, and A. G. Williams, Next-to-minimal SOFTSUSY, Comput. Phys. Commun. **185**, 2322 (2014).
[42] P. Athron, J.-h. Park, D. Stöckinger, and A. Voigt, FlexibleSUSY—A spectrum generator generator for supersymmetric models, Comput. Phys. Commun. **190**, 139 (2015).
[43] M. D. Goodsell, S. Liebler, and F. Staub, Generic calculation of two-body partial decay widths at the full one-loop level, arXiv:1703.09237.
[44] G. Belanger, V. Bizouard, F. Boudjema, and G. Chalons, One-loop renormalization of the NMSSM in SloopS: The neutralino-chargino and sfermion sectors, Phys. Rev. D **93**, 115031 (2016).
[45] N. Baro, F. Boudjema, and A. Semenov, Automatized full one-loop renormalization of the MSSM. I. The Higgs sector, the issue of $\tan\beta$ and gauge invariance, Phys. Rev. D **78**, 115003 (2008).
[46] N. Baro and F. Boudjema, Automatized full one-loop renormalization of the MSSM. II. The chargino-neutralino sector, the sfermion sector, and some applications, Phys. Rev. D **80**, 076010 (2009).
[47] N. Baro, F. Boudjema, and A. Semenov, Full one-loop corrections to the relic density in the MSSM: A few examples, Phys. Lett. B **660**, 550 (2008).
[48] N. Baro, G. Chalons, and S. Hao, Coannihilation with a chargino and gauge boson pair production at one-loop, AIP Conf. Proc. **1200**, 1067 (2010).
[49] N. Baro, F. Boudjema, G. Chalons, and S. Hao, Relic density at one-loop with gauge boson pair production, Phys. Rev. D **81**, 015005 (2010).
[50] A. Semenov, LanHEP: A package for automatic generation of Feynman rules from the Lagrangian, Comput. Phys. Commun. **115**, 124 (1998).
[51] A. Semenov, LanHEP: A package for the automatic generation of Feynman rules in field theory. Version 3.0, Comput. Phys. Commun. **180**, 431 (2009).
[52] A. Semenov, LanHEP—a package for automatic generation of Feynman rules from the Lagrangian. Updated version 3.2, Comput. Phys. Commun. **201**, 167 (2016).
[53] T. Hahn, Generating Feynman diagrams and amplitudes with FeynArts 3, Comput. Phys. Commun. **140**, 418 (2001).
[54] T. Hahn and M. Perez-Victoria, Automatized one loop calculations in four-dimensions and D-dimensions, Comput. Phys. Commun. **118**, 153 (1999).
[55] T. Hahn, Automatic loop calculations with FeynArts, FormCalc, and LoopTools, Nucl. Phys. B, Proc. Suppl. **89**, 231 (2000).
[56] G. Chalons and A. Semenov, Loop-induced photon spectral lines from neutralino annihilation in the NMSSM, J. High Energy Phys. 12 (2011) 055.
[57] G. Chalons, M. J. Dolan, and C. McCabe, Neutralino dark matter and the Fermi gamma-ray lines, J. Cosmol. Astropart. Phys. 02 (2013) 016.
[58] G. Chalons and F. Domingo, Analysis of the Higgs potentials for two doublets and a singlet, Phys. Rev. D **86**, 115024 (2012).
[59] G. Belanger, V. Bizouard, and G. Chalons, Boosting Higgs boson decays into gamma and a Z in the NMSSM, Phys. Rev. D **89**, 095023 (2014).
[60] T. Fritzsche and W. Hollik, Complete one loop corrections to the mass spectrum of charginos and neutralinos in the MSSM, Eur. Phys. J. C **24**, 619 (2002).
[61] W. Hollik and H. Rzehak, The Sfermion mass spectrum of the MSSM at the one loop level, Eur. Phys. J. C **32**, 127 (2003).
[62] G. Belanger, F. Boudjema, J. Fujimoto, T. Ishikawa, T. Kaneko, K. Kato, and Y. Shimizu, Automatic calculations in high energy physics and Grace at one-loop, Phys. Rep. **430**, 117 (2006).
[63] W. Hollik, E. Kraus, M. Roth, C. Rupp, K. Sibold, and D. Stockinger, Renormalization of the minimal supersymmetric standard model, Nucl. Phys. **B639**, 3 (2002).
[64] G. Passarino and M. J. G. Veltman, One loop corrections for e^+e^- annihilation into $\mu^+\mu^-$ in the Weinberg model, Nucl. Phys. **B160**, 151 (1979).
[65] P. H. Chankowski, S. Pokorski, and J. Rosiek, Complete on-shell renormalization scheme for the minimal supersymmetric Higgs sector, Nucl. Phys. **B423**, 437 (1994).
[66] A. Dabelstein, The one loop renormalization of the MSSM Higgs sector and its application to the neutral scalar Higgs masses, Z. Phys. C **67**, 495 (1995).
[67] Y. Yamada, Two loop renormalization of $\tan\beta$ and its gauge dependence, Phys. Lett. B **530**, 174 (2002).
[68] A. Freitas and D. Stockinger, Gauge dependence and renormalization of $\tan\beta$ in the MSSM, Phys. Rev. D **66**, 095014 (2002).
[69] V. Bizouard, Precision calculations in the next-to-minimal supersymmetric Standard Model, Ph.D. thesis, Université Grenoble Alpes, 2015; https://hal.archives-ouvertes.fr/tel-01447488.